

Accepted Manuscript

Synthesis and biological evaluation of 2,3-dihydroimidazo[1,2-*a*]benzimidazole derivatives against *Leishmania donovani* and *Trypanosoma cruzi*

Sangmi Oh, Sungbum Kim, Sunju Kong, Gyongseon Yang, Nakyung Lee, Dawoon Han, Junghyun Goo, Jair L. Siqueira-Neto, Lucio H. Freitas-Junior, Rita Song



PII: S0223-5234(14)00645-X

DOI: [10.1016/j.ejmech.2014.07.038](https://doi.org/10.1016/j.ejmech.2014.07.038)

Reference: EJMECH 7159

To appear in: *European Journal of Medicinal Chemistry*

Received Date: 6 December 2013

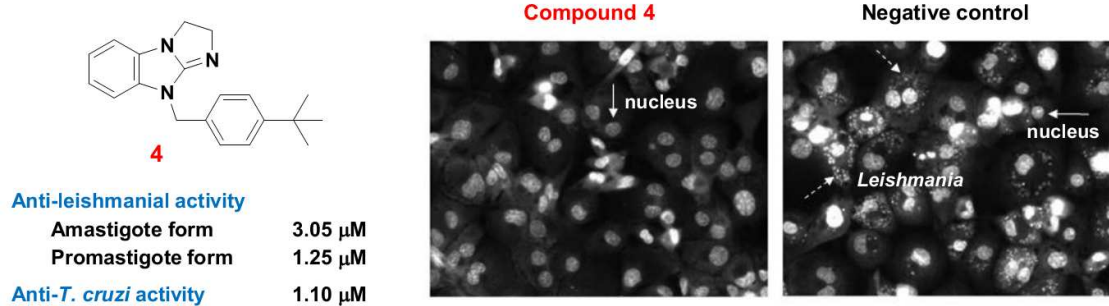
Revised Date: 9 July 2014

Accepted Date: 10 July 2014

Please cite this article as: S. Oh, S. Kim, S. Kong, G. Yang, N. Lee, D. Han, J. Goo, J.L. Siqueira-Neto, L.H. Freitas-Junior, R. Song, Synthesis and biological evaluation of 2,3-dihydroimidazo[1,2-*a*]benzimidazole derivatives against *Leishmania donovani* and *Trypanosoma cruzi*, *European Journal of Medicinal Chemistry* (2014), doi: 10.1016/j.ejmech.2014.07.038.

This is a PDF file of an unedited manuscript that has been accepted for publication. As a service to our customers we are providing this early version of the manuscript. The manuscript will undergo copyediting, typesetting, and review of the resulting proof before it is published in its final form. Please note that during the production process errors may be discovered which could affect the content, and all legal disclaimers that apply to the journal pertain.

Graphical Abstract



2,3-Dihydroimidazo[1,2-*a*]benzimidazole derivatives were synthesized and evaluated against *Leishmania donovani* and *Trypanosoma cruzi*.

Synthesis and biological evaluation of 2,3-dihydroimidazo[1,2-*a*]benzimidazole derivatives against *Leishmania donovani* and *Trypanosoma cruzi*

Sangmi Oh,^a Sungbum Kim,^a Sunju Kong,^a Gyongseon Yang,^b Nakyung Lee,^b Dawoon Han,^b
Junghyun Goo,^b Jair L. Siqueira-Neto,^{b,†} Lucio H. Freitas-Junior,^{b,‡} Rita Song^{a,*}

^a Medicinal Chemistry Group, Institut Pasteur Korea, 696 Sampyeong-dong, Bundang-gu, Seongnam-si, Gyeonggi-do 463-400, Korea

^b Center for Neglected Diseases Drug Discovery (CND3), Institut Pasteur Korea, 696 Sampyeong-dong, Bundang-gu, Seongnam-si, Gyeonggi-do 463-400, Korea

[†] Present address: University of California, San Francisco, USA

[‡] Present address: Laboratório Nacional de Biociências (LNBio), Brazil

* Corresponding author. Tel.: +82-31-8018-8230; fax: +82-31-8018-8014; e-mail: rsong@ip-korea.org

Abstract

A high-throughput (HTS) and high-content screening (HCS) campaign of a commercial library identified 2,3-dihydroimidazo[1,2-*a*]benzimidazole analogues as a novel class of anti-parasitic agents. A series of synthetic derivatives were evaluated for their *in vitro* anti-leishmanial and anti-trypanosomal activities against *L. donovani* and *T. cruzi*, which have been known as the causative parasites for visceral leishmaniasis and Chagas disease, respectively. In the case of *Leishmania*, the compounds were tested in both intracellular amastigote and extracellular promastigote assays. Compounds **4** and **24** showed promising anti-leishmanial activity against intracellular *L. donovani* (3.05 and 5.29 μ M, respectively) and anti-trypanosomal activity against *T. cruzi* (1.10 and 2.10 μ M, respectively) without serious cytotoxicity toward THP-1 and U2OS cell lines.

Keywords:

Leishmaniasis

Chagas disease

Anti-parasitic activity

2,3-Dihydroimidazo[1,2-*a*]benzimidazole

1. Introduction

The kinetoplastids are a group of flagella protozoan parasites which contain subcellular structure known as the kinetoplast as the major distinguishing feature of parasites [1]. Three distinct kinetoplastids are known to cause different human diseases: leishmaniasis caused by *Leishmania*, Chagas disease caused by *Trypanosoma cruzi* (*T. cruzi*), and sleeping sickness caused by *Trypanosoma brucei*. Among them, leishmaniasis is the most prevalent in the world found in about 88 countries affecting more than 12 million people worldwide [2], and visceral leishmaniasis caused by *Leishmania donovani* (*L. donovani*) is the most severe form of three types of leishmaniasis being mortal if left untreated [3,4]. In the case of Chagas disease, it has been found mainly in endemic areas of Latin American countries, and over 8 million people are estimated to be infected with *T. cruzi* [4]. In spite of high unmet medical needs, the molecular basis and pathway for the diseases caused by the kinetoplastids have been little elucidated and only very few target proteins have been reported [5].

Treatment options for visceral leishmaniasis are including the use of pentavalent antimonials, amphotericin B, paromomycin, and miltefosine. Although several drugs are available in the clinic for the treatment of leishmaniasis and Chagas disease, most of drugs have been faced with many difficulties such as low efficacy, severe side effects, inconvenient administration, and emergence of drug resistance [6]. For example, miltefosine is the only oral drug for the treatment of resistant leishmaniasis but this drug is teratogenic and causes extremely severe gastrointestinal side effects [7]. Likewise, nifurtimox and benznidazole have been used for the treatment of Chagas disease, but both drugs have also been reported to show limited effectiveness for the treatment of chronic patients and undesirable side effects [8]. Therefore, identification and optimization of novel anti-parasitic compounds with new mechanisms of action are urgently needed to overcome the current situation and eventually eradicate these fatal diseases.

For the discovery of novel anti-parasitic compounds, drugable targets of the pathogenic parasite have not been fully exploited so that traditional target-based drug discovery approaches become more likely to be inefficient. Only a few targets such as topoisomerases [9], kinetoplast [10], trypanothione reductase (TryR) [11], and fatty acid and sterol biosynthesis pathways [12] have been reported.

Nalidixic acid, which is the first synthetic quinolone antibiotics, has been known to have inhibitory effect on the proliferation of kinetoplastids by the inhibition of topoisomerase II [13,14]. On the other hand, other quinolone antibacterial compounds have been reported to induce a defect on kinetoplast segregation, which was not due to the topoisomerase II inhibition mechanism [15]. In addition, 2-iminobenzimidazole derivatives have been reported as a new class of TryR inhibitors [16,17], and numerous antifungal azole compounds have shown to effectively inhibit the ergosterol biosynthesis which is a key process for the formation of protozoal membrane [18,19]. However, no success in the drug discovery has been achieved so far based on the targets above mentioned, which have attracted more attention for the validation of these targets and exploitation of novel targets. Target-free cell-based assays have been widely used, as they bypass the need for a known target and have the potential to lead to the discovery of unknown target. For instance, Genomic Institute of the Novartis Research Foundation (GNF) and some laboratories supported by the Special Programme for Research and Training in Tropical Disease (TDR/WHO) have performed phenotypic screening to identify novel anti-parasitic compounds [20]. In this context, we previously reported a HTS and high-content screening (HCS) of commercially available chemical libraries against *L. donovani* [21]. Here, we report structure-activity relationship (SAR) studies of 2,3-dihydroimidazo[1,2-*a*]benzimidazole derivatives identified through phenotypic screening of 200,000 chemical library against *L. donovani* and *T. cruzi*.

2. Result and discussion

2.1. Synthesis of 2,3-dihydroimidazo[1,2-*a*]benzimidazole derivatives

General synthetic route for 2,3-dihydroimidazo[1,2-*a*]benzimidazole derivatives was depicted in **Scheme 1**. For the search of compounds with improved anti-leishmanial and anti-trypanosomal activities, SAR studies of 2,3-dihydroimidazo[1,2-*a*]benzimidazole derivatives were conducted with the modification of three different parts: tricyclic ring, substitution in benzene ring (R^1 and R^2), and substitution in imidazole nitrogen (R^3). Intermediates **1c** having benzimidazolone bicyclic ring were obtained by *N*-alkylation of aniline moiety of commercially available 2-nitroaniline derivatives (**1a**)

and then nitro reduction (**1b**), followed by intramolecular ring formation in the presence of urea [22]. These benzimidazolone compounds were chlorinated with POCl₃ and catalytic amount of HCl to give *N*-alkylated 2-chlorobenzimidazole intermediates **1d** [23]. Alternatively, in the case of compounds without substituent in the benzimidazole ring (R¹ = R² = H), **1d** was easily synthesized by reacting commercially available 2-chlorobenzimidazole with various alkyl bromide in the presence of organic base, DIPEA. Compounds **1e**, key intermediates for the tricyclic ring formation, were obtained by nucleophilic substitution with ethanolamine under microwave irradiation. After alcohol group was converted to chloride under POCl₃ condition, intramolecular cyclization in the presence of TEA was performed to yield final compounds **4** and **7–33** [24,25].

Synthesis of compound **6** containing a phenacyl substituent in benzimidazole nitrogen was started from the reaction of 2-chlorobenzimidazole with 2-bromo-4'-*tert*-butylacetophenone in the presence of base to yield **2a** (see Route I in **Scheme 2**). However, the reaction of *N*-phenacylated 2-chlorobenzimidazole **2a** with ethanolamine was failed to produce **2c**, a key intermediate for the final tricyclic compound. Due to the harsh reaction condition using microwave irradiation at 200 °C, tricyclic byproduct **2** was formed *via* intramolecular enamine formation. Therefore, **2c** was obtained by substitution reaction of 2-chlorobenzimidazole with ethanolamine and then subsequent *N*-alkylation with phenacyl bromide (see Route II in **Scheme 2**). Chlorination of alcohol moiety (**2d**) and intramolecular substitution reaction gave the final tricyclic compound **6**. All final compounds newly synthesized (**6–12**, **14–18**, **21–33**) were characterized by melting point, low resolution ESI mass and ¹H NMR.

2.2. Biological evaluation against *L. donovani*

For assessing anti-leishmanial activity of the compounds, *L. donovani* in two different stages of the life cycle was used. Intracellular amastigote form is specifically found in the host cell, and the other extracellular promastigote form is predominately found in the insect vector. Promastigotes or axenic amastigotes have been generally used in the screening for the discovery of anti-leishmanial drug candidates because of easier adaptation to the high-throughput assay format. In this study, newly

synthesized 2,3-dihydroimidazo[1,2-*a*]benzimidazole derivatives were tested in *in vitro* intracellular amastigote assays as well as extracellular promastigote, because amastigotes are substantially different from promastigotes in a molecular perspective and known to be more physiologically relevant parasite stage to evaluate anti-leishmanial activity of the compounds.

The amastigote assay was established by using metacyclic promastigote of *L. donovani* to infect differentiated THP-1 macrophages. Amastigotes transformed from metacyclic promastigotes were allowed to multiply inside host macrophages for 24 h and then the compounds were added. The quantification of the infection ratio was done 3 days after compound treatment. Fluorescent images of DNA-stained cells were acquired using automated confocal microscopy and customized software developed for image analysis allowed to assess diverse information such as number of cells per well, number of parasites per cell, infection ratio, and cell cytoplasmic area. Cytotoxicity against host cells was also easily determined by counting cell number in the same assay. Viability of promastigotes were independently accessed by fluorometric measurement of resazurin reduction after the treatment of extracellular promastigotes with each compound. *In vitro* anti-leishmanial activity of the synthesized compounds was summarized in Table 1 and 2.

As shown in Table 1, compound **4** with *para*-^{tert}butylphenyl moiety at R³ position was found to be the most active among all the synthesized compounds with EC₅₀ value of 3.05 μM which is comparable to that of the reference drug, miltefosine (4.83 μM). In addition, compound **4** didn't show any cytotoxicity against host macrophages (CC₅₀ > 50 μM) resulting in high selectivity index (SI > 16.4) while that of miltefosine was 3.91. 2,3-Dihydroimidazo[1,2-*a*]benzimidazole tricyclic ring is essential for anti-leishmanial activity because when this tricyclic ring was changed to 6-membered tetrahydropyrimidine conjugated tricyclic ring, 2,3,4,10-tetrahydropyrimido[1,2-*a*]benzimidazole (**5**) or 2,3-dihydroimidazo[1,2-*a*]benzimidazol-2-one (**3**), the anti-amastigote activity was found to be less (12.5 μM) or disappeared (> 50 μM), respectively. Phenyl group at R³ position is also critical for anti-leishmanial activity because phenacyl-substituted compound **6** and benzyl-substituted compound **8** showed decreased activities (39.4 and 25.3 μM, respectively) compared to compound **4**. In the case of compound **7** bearing phoxymethyl substituent in R³ position showed not only low anti-amastigote

activity (27.4 μM) but also cytotoxicity toward host macrophages in the similar concentration (33.1 μM).

A series of compounds described in Table 2 were synthesized to determine substituent effects of benzene included in the tricyclic ring (R^1 and R^2) and phenyl in R^3 position. Different substituents at R^1 and R^2 such as fluoro (**9**), chloro (**10**), or methyl (**11** and **12**) instead of hydrogen (**4**) were not effective to improve anti-leishmanial activity. In addition, some of the compounds (**10** and **11**) were toxic toward host macrophages even though they maintained good anti-promastigote activities (2.22 and 1.80 μM , respectively). Only fluoro-substituted compound **9** exhibited moderate activity (14.0 μM) without cytotoxicity.

Concerning substituent effect at R^3 position, potency and selectivity index were influenced by the position of the substituents and physicochemical properties such as size, electronic effect and lipophilicity. A significant decrease of anti-leishmanial activity was observed when *tert*-butyl group was changed from *para* to *meta* position (**18**) of the phenyl ring in R^3 . The presence of hydrophobic and sterically hindered substituent in *para* position such as *tert*-butyl (**4**), cyclohexyl (**16**), or phenyl (**24**) was also necessary to retain anti-parasitic activities, while the compounds with hydrogen (**13**), ethyl (**14**), and *iso*-propyl (**15**) as well as other compounds containing electron withdrawing group at *para* position (**19–23**) showed significant loss of activity. In the case of compound **24** bearing biphenylmethyl substituent, the anti-amastigote activity (5.29 μM) was comparable to that of miltefosine and selectivity index (7.5) was superior to miltefosine. To study substituent effects on biphenyl ring in R^3 , compounds **25–31** were prepared and evaluated their biological activities. However, most of compounds didn't show any improvement in terms of activity and cytotoxicity.

New compounds showing promising anti-amastigote activities in cell-based assay also revealed good anti-promastigote activities in extracellular promastigote assay. In particular, compounds **4** and **24** exhibiting anti-amastigote activities comparable to that of miltefosine in cell-based assay showed better anti-promastigote activities (1.25 and 1.48 μM , respectively) than that of miltefosine (11.1 μM). These results led us to speculate that the major target of these compounds might be in common

pathway of both stages of parasites, which allows of further target identification approaches using extracellular promastigotes more prone to handle.

Automated confocal microscopic images for the representative compounds **4** and **15** are shown in **Fig. 1**. In the case of compound **4**, no parasite was observed inside of host THP-1 cells as seen in reference drugs, miltefosine and amphotericin B, at the concentration of 12.5 μM . However, most of parasites still remained at the same concentration when they were treated with inactive compound **15**. Confocal images clearly show that no serious decrease of cell number was detected when THP-1 cells were treated with both compounds **4** and **15**. The calculated percentage of infection based on the EC_{100} of amphotericin B, which is the first effective concentration to reach 100 % activity determined as 4 μM and 1 % DMSO (0 % activity as maximum infection ratio) was normalized for the activity. Cytotoxicity was determined by percentage of cell number normalized against DMSO control.

2.3. Biological evaluation against *T. cruzi*

All compounds tested against *L. donovani* were also phenotypically screened for their *in vitro* anti-parasitic activity against *T. cruzi*. For the image-based assay, U2OS cells were used as host cells and infected with tissue culture trypomastigotes (TCT) of *T. cruzi*. In the field of drug discovery for Chagas disease, colorimetric assay using recombinant *T. cruzi* modified to express fluorescent β -galactosidase is one of the popular HTS methods to find active compounds [26]. However, wild-type *T. cruzi* was used in this study to improve the relevance between *in vitro* assay and real disease state, avoiding using genetically modified parasites [27].

In vitro anti-*T. cruzi* activity of the synthesized compounds was described in Table 3. Structure-activity relationship of 2,3-dihydroimidazo[1,2-*a*]benzimidazole derivatives against *T. cruzi* was very similar to that against *L. donovani*. The most active compound **4** in *L. donovani* assay also showed the best activity toward *T. cruzi* with an EC_{50} value of 1.10 μM and selectivity index of 33.2. Other compounds such as 6-membered tetrahydropyrimidine-conjugated tricyclic compound (**5**), fluoro-substituted compound in R^1 position (**9**), and biphenyl-substituted compound in R^3 position (**24**), which showed moderate anti-leishmanial activities (12.5, 14.0, and 5.29 μM , respectively), also

exhibited good anti-trypanosomal activities against *T. cruzi* (3.09, 8.24, and 2.10 μM , respectively). Moreover, their cytotoxicity determined in the same assay using U2OS cell lines were very low leading to high selectivity indexes.

The representative confocal images of *T. cruzi* infected cells during the assay were shown in **Fig. 2**. DNA of host cells and parasites stained by fluorescent dye was very clearly shown to be able to differentiate each other so that the anti-parasitic activity was determined by quantifying parasitemia in the presence of each compound. Benznidazole was used as a reference drug for positive control at the concentration of 400 μM , while 1 % of DMSO was used as a negative control. Even though the parasites were completely disappeared from the host cells at the concentration of 400 μM , some parasites still remained when 12.5 μM of benznidazole was treated ($\text{EC}_{50} = 20.7 \mu\text{M}$). However, in the case of compound **4** which showed the best anti-parasitic activity in this assay ($\text{EC}_{50} = 1.10 \mu\text{M}$), no parasite was observed in the host cells even at the concentration of 6.25 μM . Compound **4** showed dose-dependent clearance of the parasites from the host cells.

3. Conclusions

A series of 2,3-dihydroimidazo[1,2-*a*]benzimidazole derivatives were identified as a novel class of anti-parasitic agents. The synthetic analogues were evaluated for their *in vitro* anti-leishmanial and anti-trypanosomal activities against *L. donovani* and *T. cruzi*, respectively, which have been known as the causative protozoa for visceral leishmaniasis and Chagas disease. In the case of *Leishmania*, the compounds were tested in both intracellular amastigote and extracellular promastigote assays. Analysis of the structure-activity relationship revealed that 2,3-dihydroimidazo[1,2-*a*]benzimidazole tricyclic ring and sterically hindered hydrophobic substituent in *para*-position of benzyl group played a critical role to show anti-parasitic activity and selectivity. Compounds **4** and **24** showed promising anti-parasitic activities against *L. donovani* and *T. cruzi* without serious cytotoxicity toward human THP-1 and U2OS cell lines resulting in high selectivity indexes. A follow-up studies including optimization of anti-parasitic activity, evaluation of *in vivo* efficacy, and elucidation of mechanism of action are currently underway.

4. Experimental section

4.1. Chemistry

^1H and ^{13}C NMR spectra were recorded on a Varian High Resolution FT-NMR Spectrometer-400, and chemical shifts were measured in ppm relative to internal tetramethylsilane (TMS) standard or specific solvent signal. Routine mass analyses were performed on Waters LC/MS ZQ2000 system equipped with a reverse phase column (XBridgeTM C18 \times 3.5 μm , 50 \times 2.1 mm) and photodiode array detector using electron spray ionization (ESI). Melting point analysis was performed on BUCHI Melting point M-565. Most of reagents used in the synthetic procedure were purchased from Sigma-Aldrich, Alfa Aesar, and TCI. The progress of reaction was monitored using thin-layer chromatography (TLC) (silica gel 60 F₂₅₄, 0.25 mm), and the products were visualized by UV light (254 and 365 nm) or by ninhydrin staining followed by heating. Silica gel 60 (0.040–0.063 mm) used in flash column chromatography was purchased from Merck. Other solvents and organic reagents were purchased from commercial vendors and used without further purification unless otherwise mentioned.

4.1.1. Synthetic procedure for N-alkylation (**1a**)

To a stirred mixture of 2-nitroaniline compound (1.0 eq.) and K_2CO_3 (1.3 eq.) in dimethylformamide was added dropwise $\text{R}^3\text{CH}_2\text{Br}$ (1.3 eq.). The reaction mixture was heated to 120 °C and stirred for 4 h. After the reaction was completed, the reaction mixture was diluted with ethyl acetate and washed with water. The organic layer was dried over Na_2SO_4 and concentrated *in vacuo*. The crude product was purified by flash column chromatography (ethyl acetate / hexane) to give desired product **1a**.

4.1.2. Synthetic procedure for nitro reduction (**1b**)

To a stirred solution of **1a** (1.0 eq.) in MeOH was added 10 % Pd/C (10 % w/w). The reaction mixture was stirred for 3 h at room temperature under H_2 environment. After the reaction was completed, the reaction mixture was filtered and then concentrated *in vacuo*. The crude product was purified by flash column chromatography (ethyl acetate / hexane) to give desired product **1b**.

4.1.3. Synthetic procedure for bicyclic ring formation (**1c**)

To a stirred solution of **1b** (1.0 eq.) in dimethylformamide was added urea (2.0 eq.). The reaction mixture was heated to 200 °C and stirred for 30 min. After the reaction was completed, the reaction mixture was diluted with water and extracted with ethyl acetate. The organic layer was washed with brine, dried over Na₂SO₄ and concentrated *in vacuo*. The crude product was suspended in hexane and filtered to give desired product **1c**.

4.1.4. Synthetic procedure for chlorination (**1d**)

To a stirred solution of **1c** (1.0 eq.) and POCl₃ (10 eq.) was added a few drops of conc. HCl. The reaction mixture was heated to 150 °C and stirred for 3 h. After the reaction was completed, the reaction mixture was poured into ice water, neutralized with 1N aq. NaOH and extracted with ethyl acetate. The organic layer was washed with water, dried over Na₂SO₄ and concentrated *in vacuo* to give crude product **1d**.

Alternatively, to a stirred mixture of 2-chlorobenzimidazole (1.0 eq.) and R³CH₂Br (1.0 eq.) in dimethylformamide was added *N,N*-diisopropylethylamine (1.5 eq.). The reaction mixture was heated to 110 °C and stirred for 12 h. After the reaction was completed, the reaction mixture was cooled down to room temperature, diluted with ethyl acetate and washed with water. The organic layer was dried over anhydrous MgSO₄ and concentrated *in vacuo*. The crude product was purified by flash column chromatography (ethyl acetate / hexane) to give desired product **1d**.

4.1.5. Synthetic procedure for substitution reaction (**1e**)

A mixture of **1d** (1.0 eq.) and ethanolamine (10 eq.) was heated to 150 °C for 30 min by use of microwave irradiation. After the reaction was completed, the reaction mixture was cooled down to room temperature. The precipitated solid was filtered and washed with diethyl ether. The crude product was purified by flash column chromatography (MeOH / methylene chloride) to give desired product **1e**.

4.1.6. Synthetic procedure for chlorination (**1f**)

A mixed solution of **1e** (1.0 eq.) and POCl₃ (10 eq.) was heated to 110 °C and stirred for 2 h. After the reaction was completed, the reaction mixture was cooled down to 0 °C, quenched with ice water and extracted with ethyl acetate. The organic layer was dried over anhydrous MgSO₄ and concentrated *in vacuo*. The crude product was purified by flash column chromatography (MeOH / methylene chloride) to give desired product **1f**.

4.1.7. Synthetic procedure for intramolecular cyclization for 2,3-dihydroimidazo[1,2-a]benzimidazole derivatives (**7–12**, **14–19**, **22–32**)

To a stirred solution of **1f** (1.0 eq.) in toluene was added triethylamine (1.0 eq.). The reaction mixture was heated to 110 °C and stirred for 8 h. After the reaction was completed, the reaction mixture was cooled down to room temperature and diluted with ethyl acetate. This organic layer was washed with water, dried over anhydrous MgSO₄ and concentrated *in vacuo*. The crude product was purified by flash column chromatography (MeOH / methylene chloride) to give desired product.

4.1.7.1. 9-(4-*tert*-Butylphenoxyethyl)-2,3-dihydroimidazo[1,2-a]benzimidazole (**7**)

Yellow oil; ¹H NMR (400 MHz, CDCl₃) δ 7.26 (s, 1H), 7.24 (s, 1H), 7.07–7.05 (m, 1H), 6.98–6.96 (m, 2H), 6.79 (d, *J* = 8.8 Hz, 2H), 6.74–6.72 (m, 1H), 4.31–4.25 (m, 4H), 4.20 (t, *J* = 5.2 Hz, 2H), 3.89 (t, *J* = 8.4 Hz, 2H), 1.26 (s, 9H); LRMS (electrospray) *m/z* (M+H)⁺ 336.

4.1.7.2. 9-(4-(*tert*-Butyl)phenethyl)-2,9-dihydro-3H-benzo[*d*]imidazo[1,2-a]imidazole (**8**)

Yellow oil; ¹H NMR (400 MHz, CD₃OD) δ 7.26 (d, *J* = 6.4 Hz, 2H), 7.13 (d, *J* = 8.8 Hz, 2H), 6.95–6.91 (m, 1H), 6.87 (t, *J* = 7.8 Hz, 1H), 6.82 (d, *J* = 6.4 Hz, 1H), 6.74 (d, *J* = 8.0 Hz, 1H), 4.16 (t, *J* = 8.0 Hz, 2H), 3.97 (t, *J* = 7.2 Hz, 2H), 3.89 (t, *J* = 8.4 Hz, 2H), 2.97 (t, *J* = 7.4 Hz, 2H), 1.26 (s, 9H); LRMS (electrospray) *m/z* (M+H)⁺ 320.

4.1.7.3. 9-(4-(*tert*-Butyl)benzyl)-6-fluoro-2,9-dihydro-3H-benzo[d]imidazo[1,2-a]imidazole (**9**)

Brown solid; mp = 263.8 °C; ¹H NMR (400 MHz, CDCl₃) δ 7.40–7.38 (m, 6H), 7.12 (s, 1H), 5.34 (s, 2H), 4.33 (s, 4H), 1.25 (s, 9H); LRMS (electrospray) m/z (M+H)⁺ 324.

4.1.7.4. 9-(4-(*tert*-Butyl)benzyl)-6-chloro-3,9-dihydro-2H-benzo[d]imidazo[1,2-a]imidazole (**10**)

Pale brown solid; ¹H NMR (400 MHz, CD₃OD) δ 7.62–7.59 (m, 1H), 7.40–7.32 (m, 3H), 7.24–7.19 (m, 1H), 7.01–6.99 (m, 2H), 5.44 (s, 2H), 4.28 (t, *J* = 8.5 Hz, 2H), 4.05 (t, *J* = 8.5 Hz, 2H), 1.27 (s, 9H); LRMS (electrospray) m/z (M+H)⁺ 341.

4.1.7.5. 9-(4-(*tert*-Butyl)benzyl)-6-methyl-2,9-dihydro-3H-benzo[d]imidazo[1,2-a]imidazole (**11**)

Brown solid; ¹H NMR (400 MHz, CDCl₃) δ 7.34 (m, 5H), 7.25 (d, 1H), 7.06 (d, 1H), 5.27 (s, 2H), 4.32 (m, 4H), 2.37 (s, 3H), 1.24 (s, 9H); LRMS (electrospray) m/z (M+H)⁺ 320.

4.1.7.6. 9-(4-(*tert*-Butyl)benzyl)-6,7-dimethyl-3,9-dihydro-2H-benzo[d]imidazo[1,2-a]imidazole (**12**)

Pale yellow solid; ¹H NMR (400 MHz, CD₃OD) δ 7.28–7.22 (m, 4H), 7.12–7.09 (m, 1H), 6.82–6.80 (m, 1H), 5.31 (s, 2H), 4.07 (t, *J* = 8.5 Hz, 2H), 3.69 (t, *J* = 8.5 Hz, 2H), 2.31 (s, 3H), 2.26 (s, 3H), 1.35 (s, 9H); LRMS (electrospray) m/z (M+H)⁺ 334.

4.1.7.7. 9-(4-Ethylbenzyl)-2,3-dihydroimidazo[1,2-a]benzimidazole (**14**)

Yellow oil; ¹H NMR (400 MHz, CDCl₃) δ 7.31 (d, *J* = 8.0 Hz, 2H), 7.14 (d, *J* = 8.0 Hz, 2H), 7.02 (t, *J* = 7.6 Hz, 1H), 6.95 (t, *J* = 7.8 Hz, 1H), 6.85 (d, *J* = 4.8 Hz, 1H), 6.83 (d, *J* = 4.4 Hz, 1H), 5.13 (s, 2H), 4.35 (t, *J* = 8.4 Hz, 2H), 4.01 (t, *J* = 8.4 Hz, 2H), 2.60 (q, *J* = 7.5 Hz, 2H), 1.19 (t, *J* = 5.6 Hz, 3H); LRMS (electrospray) m/z (M+H)⁺ 278.

4.1.7.8. 9-(4-Isopropylbenzyl)-2,9-dihydro-3H-benzo[d]imidazo[1,2-a]imidazole (**15**)

White solid; mp = 133.2 °C; ¹H NMR (400 MHz, CD₃OD) δ 7.44 (d, *J* = 8.4 Hz, 1H), 7.39–7.31 (m, 3H), 7.28–7.22 (m, 2H), 7.18 (d, *J* = 8.0 Hz, 2H), 6.01 (s, 2H), 4.79–4.75 (m, 2H), 4.43 (t, *J* = 8.6 Hz,

2H), 2.85–2.82 (m, 1H), 1.18 (d, $J = 6.8$ Hz, 6H); LRMS (electrospray) m/z (M+H)⁺ 292.

4.1.7.9. 9-(4-Cyclohexylbenzyl)-2,9-dihydro-3H-benzo[d]imidazo[1,2-a]imidazole (**16**)

Yellow oil; ¹H NMR (400 MHz, CD₃OD) δ 7.23 (d, $J = 8.0$ Hz, 2H), 7.15 (d, $J = 8.0$ Hz, 2H), 6.97–6.93 (m, 1H), 6.89–6.80 (m, 3H), 4.94 (s, 2H), 4.20 (t, $J = 7.8$ Hz, 2H), 3.92 (t, $J = 8.0$ Hz, 2H), 2.45 (brs, 1H), 1.80–1.71 (m, 5H), 1.45–1.24 (m, 5H); LRMS (electrospray) m/z (M+H)⁺ 332.

4.1.7.10. 9-(3,5-Dimethylbenzyl)-2,9-dihydro-3H-benzo[d]imidazo[1,2-a]imidazole (**17**)

Yellow solid; mp = 274.6 °C; ¹H NMR (400 MHz, CD₃OD) δ 7.02–6.85 (m, 7H), 4.94 (s, 2H), 4.25 (t, $J = 8.6$ Hz, 2H), 4.00 (t, $J = 8.4$ Hz, 2H), 2.25 (s, 6H); LRMS (electrospray) m/z (M+H)⁺ 278.

4.1.7.11. 9-(3-(tert-Butyl)benzyl)-2,9-dihydro-3H-benzo[d]imidazo[1,2-a]imidazole (**18**)

White solid; mp = 248.6 °C; ¹H NMR (400 MHz, CDCl₃) δ 7.34 (m, 5H), 7.25 (d, 1H), 7.06 (d, 1H), 7.17 (m, 3H), 5.27 (s, 2H), 4.32 (m, 4H), 1.24 (s, 9H); LRMS (electrospray) m/z (M+H)⁺ 306.

4.1.7.12. 9-(4-(Methylsulfonyl)benzyl)-2,9-dihydro-3H-benzo[d]imidazo[1,2-a]imidazole (**19**)

Yellow solid; mp = 149.5 °C; ¹H NMR (400 MHz, CD₃OD) δ 7.93 (d, $J = 8.0$ Hz, 2H), 7.59 (d, $J = 8.0$ Hz, 2H), 7.04–6.87 (m, 4H), 5.15 (s, 2H), 4.24 (t, $J = 8.2$ Hz, 2H), 4.01 (t, $J = 8.6$ Hz, 2H), 3.09 (s, 3H); LRMS (electrospray) m/z (M+H)⁺ 328.

4.1.7.13. 9-(4-(Trifluoromethoxy)benzyl)-3,9-dihydro-2H-benzo[d]imidazo[1,2-a]imidazole (**22**)

White solid; mp = 183.9 °C; ¹H NMR (400 MHz, CD₃OD) δ 7.93–7.91 (m, 2H), 7.48–7.46 (m, 2H), 7.43–7.41 (m, 1H), 7.38–7.34 (m, 2H), 7.29–7.27 (m, 2H), 5.43 (s, 2H), 4.45 (t, $J = 8.5$ Hz, 2H), 4.10 (t, $J = 8.5$ Hz, 2H). LRMS (electrospray) m/z (M+H)⁺ 334.

4.1.7.14. 9-(4-Cyanobenzyl)-3,9-dihydro-2H-benzo[d]imidazo[1,2-a]imidazole (**23**)

White solid; mp = 190.0 °C; ¹H NMR (400 MHz, CDCl₃) δ 7.45–7.42 (m, 2H), 7.26–7.23 (m, 2H), 6.97–6.84 (m, 2H), 6.75–6.65 (m, 2H), 4.95 (s, 2H), 4.29 (t, *J* = 8.5 Hz, 2H), 3.91 (t, *J* = 8.5 Hz, 2H). LRMS (electrospray) *m/z* (M+H)⁺ 275.

4.1.7.15. 9-(4-Phenylbenzyl)-2,3-dihydroimidazo[1,2-*a*]benzimidazole (24)

Yellow solid; mp = 139.5 °C; ¹H NMR (400 MHz, CDCl₃) δ 7.54 (d, *J* = 8.4 Hz, 4H), 7.44–7.40 (m, 4H), 7.33 (t, *J* = 7.4 Hz, 1H), 6.96 (t, *J* = 7.6 Hz, 1H), 6.89 (d, *J* = 7.8 Hz, 1H), 6.76 (d, *J* = 7.6 Hz, 2H), 5.30 (s, 2H), 4.29 (t, *J* = 8.6 Hz, 2H), 3.94 (t, *J* = 8.4 Hz, 2H); LRMS (electrospray) *m/z* (M+H)⁺ 326.

4.1.7.16. 9-((2',6'-Difluoro-[1,1'-biphenyl]-4-yl)methyl)-2,9-dihydro-3H-benzo[*d*]imidazo[1,2-*a*]imidazole (25)

Brown solid; mp = 210.4 °C; ¹H NMR (400 MHz, CD₃OD) δ 7.43–7.36 (m, 5H), 7.24 (d, *J* = 7.6 Hz, 1H), 7.13–7.08 (m, 3H), 7.03 (t, *J* = 7.6 Hz, 2H), 5.18 (s, 2H), 4.25 (t, *J* = 8.6 Hz, 2H), 3.04 (t, *J* = 6.4 Hz, 2H); LRMS (electrospray) *m/z* (M+H)⁺ 362.

4.1.7.17. 9-((4'-Fluoro-[1,1'-biphenyl]-4-yl)methyl)-3,9-dihydro-2H-benzo[*d*]imidazo[1,2-*a*]imidazole (26)

Brown solid; mp = 199.5 °C; ¹H NMR (400 MHz, CD₃OD) δ 7.64–7.48 (m, 4H), 7.40 (d, *J* = 8.1 Hz, 2H), 7.12 (t, *J* = 8.7 Hz, 2H), 7.02 (dd, *J* = 6.9 and 2.2 Hz, 1H), 6.94 (d, *J* = 6.2 Hz, 3H), 5.08 (s, 2H), 4.26 (t, *J* = 8.5 Hz, 2H), 4.02 (t, *J* = 8.5 Hz, 2H); LRMS (electrospray) *m/z* (M+H)⁺ 344.

4.1.7.18. 9-((4'-Methyl-[1,1'-biphenyl]-4-yl)methyl)-3,9-dihydro-2H-benzo[*d*]imidazo[1,2-*a*]imidazole (27)

Pale yellow solid; mp = 202.1 °C; ¹H NMR (400 MHz, CD₃OD) δ 7.56–7.54 (m, 2H), 7.47–7.42 (m, 2H), 7.40–7.38 (m, 2H), 7.28–7.23 (m, 2H), 7.12–7.01 (m, 1H), 6.99–6.95 (m, 3H), 5.09 (s, 2H), 4.26 (t, *J* = 8.5 Hz, 2H), 4.13 (t, *J* = 8.5 Hz, 2H), 2.34 (s, 3H); LRMS (electrospray) *m/z* (M+H)⁺ 340.

4.1.7.19. 9-((4'-Methyl-[1,1'-biphenyl]-4-yl)methyl)-3,9-dihydro-2H-benzo[d]imidazo[1,2-a]imidazole (**28**)

Pale brown solid; mp = 202.1 °C; ¹H NMR (400 MHz, CD₃OD) δ 7.77 (d, *J* = 8.3 Hz, 2H), 7.71 (d, *J* = 8.3 Hz, 2H), 7.65 (s, 2H), 7.47 (d, *J* = 8.1 Hz, 2H), 7.10–7.00 (m, 1H), 7.00–6.92 (m, 3H), 5.14 (s, 2H), 4.28 (t, *J* = 8.5 Hz, 2H), 4.07 (t, *J* = 8.5 Hz, 2H); LRMS (electrospray) *m/z* (M+H)⁺ 394.

4.1.7.20. 9-((4'-Chloro-[1,1'-biphenyl]-4-yl)methyl)-3,9-dihydro-2H-benzo[d]imidazo[1,2-a]imidazole (**29**)

Pale brown solid; mp = 198.6 °C; ¹H NMR (400 MHz, CD₃OD) δ 7.72–7.65 (m, 2H), 7.59–7.49 (m, 3H), 7.47–7.30 (m, 4H), 7.02 (s, 1H), 6.72 (d, *J* = 7.0 Hz, 2H), 5.24 (s, 2H), 4.13–4.09 (m, 2H), 3.73–3.69 (m, 2H); LRMS (electrospray) *m/z* (M+H)⁺ 361.

4.1.7.21. 9-((4'-Methoxy-[1,1'-biphenyl]-4-yl)methyl)-3,9-dihydro-2H-benzo[d]imidazo[1,2-a]imidazole (**30**)

Pale brown solid; ¹H NMR (400 MHz, CD₃OD) δ 7.67–7.58 (m, 2H), 7.58–7.54 (m, 2H), 7.53–7.44 (m, 2H), 7.42–7.39 (m, 1H), 7.07–7.00 (m, 3H), 6.83 (d, *J* = 6.1 Hz, 2H), 5.31 (s, 2H), 4.32 (t, *J* = 8.5 Hz, 2H), 3.83 (t, *J* = 8.5 Hz, 2H), 3.40 (s, 3H); LRMS (electrospray) *m/z* (M+H)⁺ 356.

4.1.7.22. 9-((4'-(Trifluoromethoxy)-[1,1'-biphenyl]-4-yl)methyl)-3,9-dihydro-2H-benzo[d]imidazo[1,2-a]imidazole (**31**)

Pale yellow solid; ¹H NMR (400 MHz, CD₃OD) δ 7.65–7.50 (m, 4H), 7.48–7.43 (m, 2H), 7.40–7.38 (m, 1H), 7.14–6.99 (m, 3H), 6.84 (d, *J* = 4.6 Hz, 2H), 5.37 (s, 2H), 4.25–3.93 (m, 2H), 3.76–3.72 (m, 2H); LRMS (electrospray) *m/z* (M+H)⁺ 410.

4.1.7.23. 9-(4-Phenoxybenzyl)-2,9-dihydro-3H-benzo[d]imidazo[1,2-a]imidazole (**32**)

Pale yellow solid; ^1H NMR (400 MHz, CD_3OD) δ 7.37–7.31 (m, 4H), 7.21–7.06 (m, 6H), 6.97–6.94 (m, 3H), 5.11 (s, 2H), 4.33–4.29 (m, 2H), 4.18–4.13 (m, 2H); LRMS (electrospray) m/z ($\text{M}+\text{H}$) $^+$ 342.

4.1.8. Synthetic procedure for substitution reaction (2-(1H-Benzo[d]imidazol-2-ylamino)ethanol, **2b**)

A mixture of 2-chloro-1H-benzo[d]imidazole (1.0 eq.) and ethanolamine (10 eq.) was heated to 200 °C for 30 min by use of microwave irradiation. After the reaction was completed, the reaction mixture was cooled down to room temperature. The precipitated solid was filtered and washed with water to give desired product **2b**. White solid (96 % yield); mp = 177.4 °C; ^1H NMR (400 MHz, CD_3OD) δ 7.20–7.18 (m, 2H), 6.97–6.95 (m, 2H), 3.75 (t, J = 5.6 Hz, 2H), 3.49 (t, J = 5.4 Hz, 2H); LRMS (electrospray) m/z ($\text{M}+\text{H}$) $^+$ 178.

4.1.9. Synthetic procedure for substitution reaction (1-(4-tert-Butylphenyl)-2-(2-(2-hydroxyethylamino)-1H-benzo[d]imidazol-1-yl)ethanone, **2c**)

To a stirred mixture of **2b** (1.0 eq.) in dimethylformamide was added 2-bromo-4-*tert*-butylacetophenone (1.0 eq.). The reaction mixture was stirred for 15 h. After the reaction was completed, the reaction mixture was diluted with distilled water. The precipitated solid was filtered, washed with distilled water and dried to give desired product **2c**. White solid (55 % yield); mp = 230.7 °C; ^1H NMR (400 MHz, CD_3OD) δ 8.09 (d, J = 6.8 Hz, 2H), 7.67 (d, J = 6.8 Hz, 2H), 7.47 (d, J = 7.6 Hz, 1H), 7.34–7.29 (m, 3H), 5.84 (s, 2H), 3.79 (t, J = 5.2 Hz, 2H), 3.59 (t, J = 5.4 Hz, 2H), 1.38 (s, 9H); LRMS (electrospray) m/z ($\text{M}+\text{H}$) $^+$ 352.

4.1.10. Synthetic procedure for substitution reaction (**2d**)

A mixed solution of **2c** (1.0 eq.) and POCl_3 (10 eq.) was heated to 110 °C and stirred for 2 h. After the reaction was completed, the reaction mixture was cooled down to 0 °C, quenched with ice water and extracted with methylene chloride. The organic layer was dried over anhydrous MgSO_4 and concentrated *in vacuo*. The crude product **2d** was used in the next step without further purification.

4.1.11. Synthetic procedure for intramolecular ring formation (9-(4-*tert*-Butylphenacyl)-2,3-dihydroimidazo[1,2-*a*]benzimidazole, **6**)

To a stirred solution of **2d** (1.0 eq.) in toluene was added triethylamine (1.0 eq.). The reaction mixture was heated to 110 °C and stirred for 8 h. After the reaction was completed, the reaction mixture was cooled down to room temperature and diluted with ethyl acetate. This organic layer was washed with water, dried over anhydrous MgSO₄ and concentrated *in vacuo*. The crude product was purified by flash column chromatography (MeOH / methylene chloride) to give desired product **6**. Yellow oil (19 % overall 2 steps yield); ¹H NMR (400 MHz, CDCl₃) δ 8.00 (d, *J* = 8.4 Hz, 2H), 7.51 (d, *J* = 8.4 Hz, 2H), 7.12 (t, *J* = 7.6 Hz, 1H), 7.05 (t, *J* = 7.8 Hz, 1H), 6.96 (d, *J* = 7.6 Hz, 1H), 6.81 (d, *J* = 7.6 Hz, 1H), 5.70 (s, 2H), 4.38 (t, *J* = 8.6 Hz, 2H), 4.15 (t, *J* = 8.4 Hz, 2H), 1.34 (s, 9H); LRMS (electrospray) *m/z* (M+H)⁺ 334.

4.2. Biology

4.2.1. Parasite and cell cultures

L. donovani parasites (MHOM/ET/67/HU3, ATCC 50127) were cultivated as promastigotes at 28 °C in M199 with 40 mM HEPES, 0.1 mM adenine, 0.0001 % biotin and 4.62 mM NaHCO₃, supplemented with 10 % heat-inactivated FBS. Parasites were sub-cultured every 2 or 3 days. THP-1 cells (ATCC TIB-202) were cultivated in RPMI supplemented with 10 % FBS at 37 °C with 5 % CO₂. Tissue culture trypomastigotes (TCT) of *T. cruzi* were maintained in LLC-MK2 cell line. Every 6–8 days after infection, TCT was released in the supernatant and re-infect LLC-MK2 cell line. LLC-MK2 and U2OS cell line were cultivated in DMEM with 10% FBS at 37 °C with 5 % CO₂.

4.2.2. Intracellular *Leishmania* (amastigote) screening assay

The screening assay for *Leishmania* was performed using previously reported protocol with slight modification in incubation period [21]. Briefly, *L. donovani* culture was incubated 6 days before infection to generate metacyclic promastigotes which is macrophage-infective form. THP-1 cells were differentiated with 50 ng/mL of phorbol 12-myristate 13-acetate (PMA, Sigma P1585) before

infection. Cells and parasites were seeded with 1:20 infection ratio in 384 well plates, using a WellMate™ liquid handler. After 24 h incubation at 37 °C with 5 % CO₂, 4 μM of reference drug amphotericin B (Sigma A2942) as EC₁₀₀ (positive control), 1 % DMSO (negative control), and the compounds were added to the wells followed by incubation at 37 °C with 5 % CO₂ for 3 days. Wells were then washed with PBS, fixed with 4 % paraformaldehyde, and then DNA was stained with DRAQ5™. Automated confocal microscope (Perkin Elmer) was used to take pictures of the plates and images were analyzed by software developed in house.

4.2.3. Extracellular *Leishmania* (promastigote) assay

L. donovani (1×10^6 parasites/mL) were seeded in 384 plate (Evotec™) containing each compound dissolved in DMSO. *Leishmania* was incubated with the compounds for 28 h and 400 μM of resazurin sodium salt (Sigma R7017) was added in the plate. After additional incubation with the compounds for 20 h, the parasites were fixed with 4 % paraformaldehyde and the plates were analyzed in Victor3™ (Perkin Elmer) at 590 nm (emission) with the excitation at 530 nm [28].

4.2.4 Intracellular *Trypanosoma cruzi* assay

Tissue culture trypomastigotes (TCT) of *T. cruzi* were obtained from metacyclic trypomastigotes after infection to LLC-MK2 cell line. U2OS cell line was used as host cells for the phenotypic assay. In the plate containing each compound, homogeneous mixture of U2OS cells and parasites was dispensed and incubated for 48 h at 37 °C with 5 % CO₂. After incubation was completed, the parasites were fixed with 4 % paraformaldehyde, and then DNA was stained with DRAQ5™. Automated confocal microscope (Perkin Elmer) was used to take pictures of the plates and then images were analyzed by software developed in house [27].

4.2.5. Data analysis

The acquired images were analyzed with in-house software to quantify cell numbers, parasites numbers, and infection ratio. 4 μM of amphotericin B for *L. donovani*, 400 μM of benznidazole for *T.*

cruzi, and 1 % of DMSO were used for positive and negative controls, respectively. 2-Fold dilution with 10 points of reference drugs were tested for assay-to-assay quality control by comparing EC_{50} and DRC graph. Collected data were used to determine the activities of synthesized compounds in terms of EC_{50} , CC_{50} and SI value. EC_{50} was calculated by infection ratio normalized by positive and negative controls. CC_{50} value was obtained from counting THP-1 and U2OS cell numbers, and SI value was determined by EC_{50}/CC_{50} value. Quality of all performed assay was controlled by Z' value, windows and CV [29].

Acknowledgements

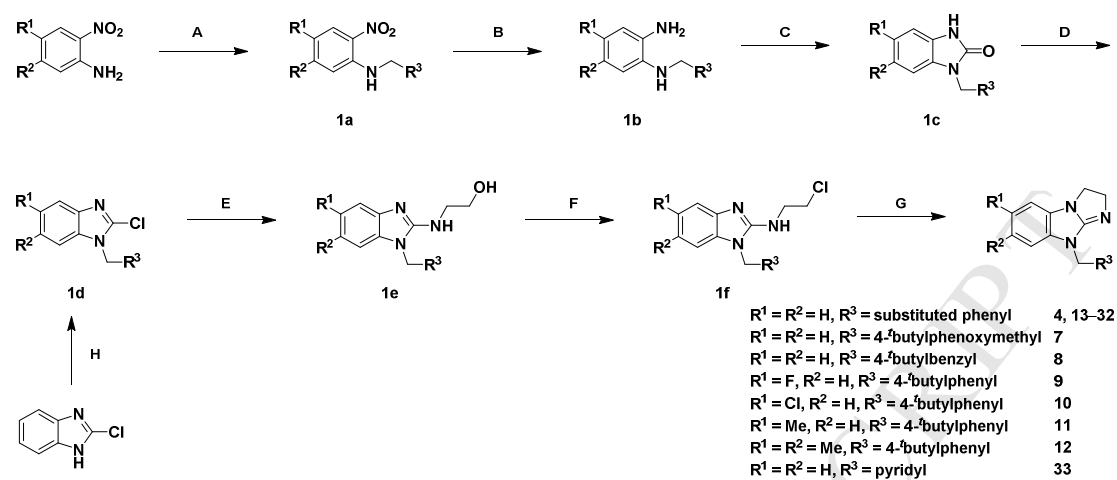
This work was supported by the National Research foundation of Korea (NRF) grant funded by the Korea government (MSIP, No. 2007-00559), Gyeonggi-do (No. K204EA000001-09E0100-00110), and KISTI.

References

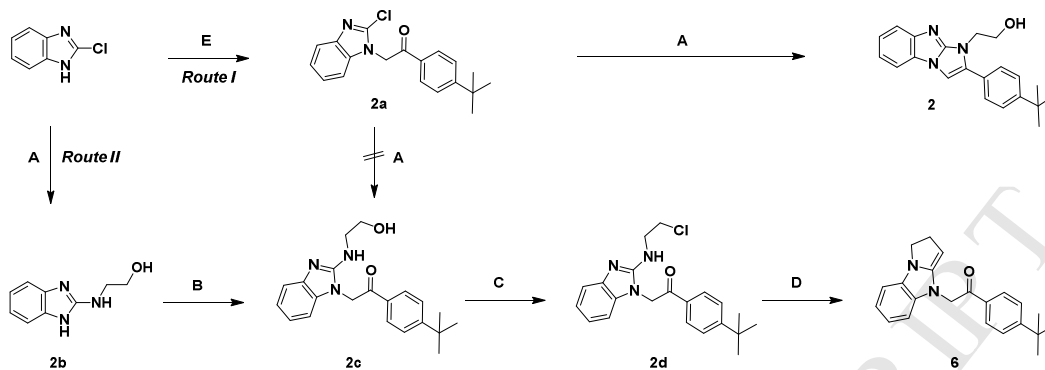
- [1] K. Stuart, R. Brun, S. Croft, A. Fairlamb, R.E. Gürtler, J. McKerrow, S. Reed, R. Tarleton, Kinetoplastids: related protozoan pathogens, different diseases, *J. Clin. Invest.* 118 (2008), 1301–1310.
- [2] R. Reithinger, J.C. Dujardin, Molecular diagnosis of leishmaniasis: current status and future applications, *J. Clin. Microbiol.* 45 (2007), 21–25.
- [3] G.G. Baily, A. Nandy, Visceral leishmaniasis: more prevalent and more problematic. *J. Infect.* 29 (1994), 241–247.
- [4] F. Chappuis, S. Sundar, A. Hailu, H. Ghalib, S. Rijal, R.W. Peeling, J. Alvar, M. Boelaert, Visceral leishmaniasis: what are the needs for diagnosis, treatment and control? *Nat. Rev. Microbiol.* 5 (2007), 873–882.
- [5] S.L. Croft, G.H. Coombs, Leishmaniasis – current chemotherapy and recent advances in the search for novel drugs, *Trends Parasitol.* 19 (2003), 502–508.
- [6] B. Purkait, A. Kumar, N. Nandi, A.H. Sardar, S. Das, S. Kumar, K. Pandey, V. Ravidas, M. Kumar, T. De, D. Singh, P. Das, Mechanism of amphotericin B resistance in clinical isolates of *Leishmania donovani*, *Antimicrob. Agents Chemother.* 56 (2012), 1031–1041.
- [7] F.J. Pérez-Victoria, S. Castanys, F. Gamarro, *Leishmania donovani* resistance to miltefosine involves a defective inward translocation of the drug, *Antimicrob. Agents Chemother.* 47 (2003), 2397–2403.
- [8] J.A. Pérez-Molina, A. Pérez-Ayala, S. Moreno, M.C. Fernández-González, J. Zamora, R. López-Velez, Use of benznidazole to treat chronic Chagas' disease: a systematic review with a meta-analysis, *J. Antimicrob. Chemother.* 64 (2009), 1139–1147.

- [9] B.B. Das, A. Ganguly, H.K. Majumder, DNA topoisomerases of *Leishmania*: the potential targets for anti-leishmanial therapy, *Adv. Exp. Med. Biol.* 625 (2008), 103–115.
- [10] M.C. Motta, Kinetoplast as a potential chemotherapeutic target of trypanosomatids, *Curr. Pharm. Des.* 14 (2008), 847–854.
- [11] R.L. Krauth-Siegel, S.K. Meiering, H. Schmidt, The parasite-specific trypanothione metabolism of *Trypanosoma* and *Leishmania*, *Biol. Chem.* 384 (2003), 539–549.
- [12] C.W. Roberts, R. McLeord, D.W. Rice, M. Ginger, M.L. Chance, L.J. Goad, Fatty acid and sterol metabolism: potential antimicrobial targets in apicomplexan and trypanosomatid parasitic protozoa, *Mol. Biochem. Parasitol.* 126 (2003), 129–142.
- [13] A. Cavalli, M.L. Bolognesi, Neglected tropical diseases: Multi-target-directed ligands in the search for novel lead candidates against *Trypanosoma* and *Leishmania*, *J. Med. Chem.* 52 (2009), 7339–7359.
- [14] D.P. Cavalcanti, S.P. Fragoso, S. Goldenberg, W. de Souza, M.C. Motta, The effect of topoisomerase II inhibitors on the kinetoplast ultrastructure, *Parasitol. Res.* 94 (2004), 439–448.
- [15] G. Hiltensperger, N.G. Jones, S. Niedermeier, A. Stich, M. Kaiser, J. Jung, S. Puhl, A. Damme, H. Braunschweig, L. Meinel, M. Engstler, U. Holzgrabe, Synthesis and structure-activity relationships of new quinolone-type molecules against *Trypanosoma brucei*, *J. Med. Chem.* 55 (2012), 2538–2548.
- [16] G.A. Holloway, J.B. Baell, A.H. Fairlamb, P.M. Novello, J.P. Parisot, J. Richardson, K.G. Watson, I.P. Street, Discovery of 2-iminobenzimidazoles as a new class of trypanothione reductase inhibitor by high-throughput screening, *Bioorg. Med. Chem. Lett.* 17 (2007), 1422–1427.
- [17] G.A. Holloway, W.N. Charman, A.H. Fairlamb, R. Brun, M. Kaiser, E. Kostewicz, P. M. Novello, J.P. Parisot, J. Richardson, I.P. Street, K.G. Watson, J.B. Baell, Trypanothione reductase high-throughput screening campaign identifies novel classes of inhibitors with antiparasitic activity, *Antimicrob. Agents Chemother.* 53 (2009), 2824–2833.
- [18] A.R. Renslo, J.H. McKerrow, Drug discovery and development for neglected parasitic diseases, *Nat. Chem. Biol.* 2 (2006), 701–710.
- [19] S.L. Croft, M.P. Barrett, J.A. Urbina, Chemotherapy of trypanosomiasis and leishmaniasis, *Trends Parasitol.* 21 (2005), 508–512.

- [20] L.H. Freitas-Junior, E. Chatelain, H.A. Kim, J.L. Siqueira-Neto, Visceral leishmaniasis treatment: What do we have, what do we need and how to deliver it? *Int. J. Parasitol. Drugs Drug Resist.* 2 (2012), 11–19.
- [21] J.L. Siqueira-Neto, S. Moon, J. Jang, G. Yang, C. Lee, H.K. Moon, E. Chatelain, A. Genovesio, J. Cechetto, L.H. Freitas-Junior, An image-based high-content screening assay for compounds targeting intracellular *Leishmania donovani* Amastigotes in human, *PLoS Negl. Trop. Dis.* 6 (2012), e1671.
- [22] R. Iemura, M. Hori, H. Ohtaka, Syntheses of the metabolites of 1-(2-ethoxyethyl)-2-(hexahydro-4-methyl-1*H*-1,4-diazepin-1-yl)-1*H*-benzimidazole difumarate (KG-2413) and related compounds, *Chem. Pharm. Bull.* 37 (1989), 962–966.
- [23] B. Buckman, J.B. Nicholas, L. Beigelman, V. Serebryany, A.D. Stoycheva, T. Thrailkill, S.D. Seiwert, Cyclic peptide inhibitors of hepatitis C virus replication, *PCT Int. Appl. WO2011038293*, 2011.
- [24] V.A. Anisimova, I.E. Tolpygin, A.A. Spasov, V.A. Kosolapov, A.V. Stepanov, A.F. Kucheryavenko, Synthesis and biological activity of *N*-acylmethyl derivatives of 9*H*-2,3-dihydroimidazo- and 10*H*-2,3,4,10-tetrahydropyrimido[1,2-*a*]benzimidazoles and their reduction products, *Pharmaceutical Chem. J.* 40 (2006), 261–267.
- [25] V.A. Anisimova, I.E. Tolpygin, G.S. Borodkin, Research in the field of imidazo[1,2-*a*]benzimidazole derivatives: XXVII. 1-Acylmethyl-2-(ω -hydroxyalkylamino)benzimidazoles and their transformation into derivatives of tricyclic systems, *Russian J. Org. Chem.* 46 (2010), 275–285.
- [26] F.S. Buckner, C.L. Verlinde, A.C. La Flamme, W.C. Van Voorhis, Efficient technique for screening drug for activity against *Trypanosoma cruzi* using parasites expressing β -galactosidase, *Antimicrob. Agents Chemother.* 40 (1996), 2592–2597.
- [27] Moon *et al.*, *PLoS one*, submitted.
- [28] J.L. Siqueira-Neto, O.-R. Song, H. Oh, J.-H. Sohn, G. Yang, J. Jang, J. Cechetto, C.B. Lee, S. Moon, A. Genovesio, E. Chatelain, T. Christophe, L.H. Freitas-Junior, Antileishmanial high-throughput drug screening reveals drug candidates with new scaffolds, *PLoS Negl. Trop. Dis.* 4 (2010), e675.
- [29] J.H. Zhang, T.D. Chung, K.R. Oldenburg, A simple statistical parameter for use in evaluation and validation of high throughput screening assays, *J. Biomol. Screen.* 4 (1999), 67–73.

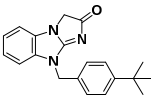
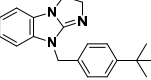
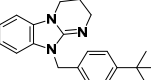
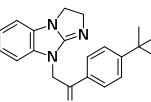
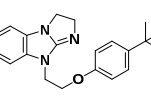
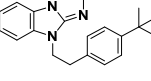


Scheme 1. Reagents and conditions: (A) R^3CH_2Br 1.3 eq, K_2CO_3 1.3 eq, DMF, 120 °C, 4 h; (B) H_2 , 10 % Pd/C, MeOH, RT, 3 h; (C) urea 2.0 eq, DMF, 200 °C, 30 min; (D) $POCl_3$ 10.0 eq, conc. HCl (cat.), 150 °C, 3 h; (E) ethanolamine 10.0 eq, microwave irradiation, 200 °C, 30 min; (F) $POCl_3$ 10.0 eq, 110 °C, 2 h; (G) TEA 1.0 eq, toluene, 110 °C, 8 h; (H) R^3CH_2Br 1.0 eq, DIPEA 1.5 eq, DMF, 100 °C, 12 h.



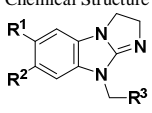
Scheme 2. Reagents and conditions: (A) Ethanolamine 10.0 eq, microwave irradiation, 200 °C, 30 min; (B) 2-bromo-4'-*tert*-butylacetophenone 1.0 eq, DMF, 15 h; (C) POCl₃ 10.0 eq, 110 °C, 2 h; (D) TEA 1.0 eq, toluene, 110 °C, 8 h; (E) 2-bromo-4'-*tert*-butylacetophenone 1.0 eq, DIPEA 1.5 eq, DMF, 100 °C, 8 h.

Table 1. *In vitro* activity of 2,3-dihydroimidazo[1,2-*a*]benzimidazole derivatives against amastigotes and promastigotes of *L. donovani*

Compound ^a	Chemical Structure	Activity against <i>L. donovani</i>			
		Amastigote form			Promastigote form
		EC ₅₀ (μM) ^b	CC ₅₀ (μM) ^c	SI ^d	EC ₅₀ (μM) ^e
3		> 50	> 50	N/A ^f	N/T ^g
4		3.05	> 50	> 16.4	1.25
5		12.5	> 50	> 3.98	2.73
6		39.4	> 50	> 1.27	NT
7		27.4	33.1	1.21	NT
8		25.3	> 50	> 1.98	20.8
Miltefosine		4.83	18.9	3.91	11.1
Amphotericin B		0.25	7.57	30.2	0.22

^a Compound 3–5 are already known molecules. ^b EC₅₀ indicates half maximal effective concentration on intracellular *L. donovani* (2-fold dilution with 10 points dose response). Average of duplicate determinations. ^c CC₅₀ indicates cytotoxicity against THP-1 cells, which was determined by counting of THP-1 cell numbers in the taken image from intracellular assay. Average of duplicate determinations. ^d SI is selective index (EC₅₀ / CC₅₀). ^e EC₅₀ indicates half maximal effective concentration on extracellular *L. donovani*. Average of duplicate determinations. ^f N/A, not available. ^g N/T, not tested.

Table 2. *In vitro* activity of 2,3-dihydroimidazo[1,2-*a*]benzimidazole derivatives against amastigotes and promastigotes of *L. donovani*

Compound ^a	Chemical Structure			Activity against <i>L. donovani</i>			
				Amastigote form			Promastigote form
	R ¹	R ²	R ³	EC ₅₀ (μM) ^a	CC ₅₀ (μM) ^b	SI ^c	EC ₅₀ (μM) ^d
4	H	H	4- <i>tert</i> -butylphenyl	3.05	> 50	> 16.4	1.25
9	F	H	4- <i>tert</i> -butylphenyl	14.0	> 50	> 3.57	1.26
10	Cl	H	4- <i>tert</i> -butylphenyl	7.33	12.5	1.71	2.22
11	Me	H	4- <i>tert</i> -butylphenyl	11.0	28.1	2.55	1.80
12	Me	Me	4- <i>tert</i> -butylphenyl	> 50	> 50	N/A	N/T
13	H	H	phenyl	> 50	> 50	N/A	N/T
14	H	H	4-ethylphenyl	42	> 50	> 1.19	N/T
15	H	H	4- <i>iso</i> -propylphenyl	> 50	> 50	N/A	N/T
16	H	H	4-cyclohexylphenyl	5.4	22.8	4.19	1.71
17	H	H	3,5-dimethylphenyl	> 50	> 50	N/A	N/T
18	H	H	3- <i>tert</i> -butylphenyl	22.6	> 50	> 2.21	4.98
19	H	H	4-methylsulfonylphenyl	> 50	> 50	N/A	N/T
20	H	H	4-fluorophenyl	> 50	> 50	N/A	N/T
21	H	H	4-trifluoromethylphenyl	> 50	> 50	N/A	N/T
22	H	H	4-trifluoromethoxyphenyl	> 50	> 50	N/A	N/T
23	H	H	4-cyanophenyl	> 50	> 50	N/A	N/T
24	H	H	4-(1,1'-biphenyl)	5.29	39.7	7.5	1.48
25	H	H	4-(2',5'-difluoro-1,1'-biphenyl)	32.5	> 50	> 1.54	9.22
26	H	H	4-(4'-fluoro-1,1'-biphenyl)	8.88	35.0	3.94	1.49
27	H	H	4-(4'-methyl-1,1'-biphenyl)	17.8	27.1	1.52	1.75
28	H	H	4-(4'-trifluoromethyl-1,1'-biphenyl)	10.3	30.0	2.91	3.11
29	H	H	4-(4'-chloro-1,1'-biphenyl)	13.7	20.0	1.46	N/T
30	H	H	4-(4'-methoxy-1,1'-biphenyl)	10.2	23.0	2.25	2.34
31	H	H	4-(4'-trifluoromethoxy-1,1'-biphenyl)	5.20	11.0	2.11	1.53
32	H	H	4-phenoxyphenyl	12.5	48.0	3.82	2.01
33	H	H	2-pyridyl	> 50	> 50	N/A	N/T
Miltefosine				4.83	18.9	3.91	11.1
Amphotericin B				0.25	7.57	30.2	0.22

^a Compound **13**, **20**, and **21** are already known molecules. ^b EC₅₀ indicate half maximal effective concentration on intracellular *L. donovani* (2-fold dilution with 10 points dose response). Average of duplicate determinations. ^c CC₅₀ indicate cytotoxicity against THP-1 cells, which was determined by counting of THP-1 cell numbers in the taken image from intracellular assay. Average of duplicate determinations. ^d SI is selective index (EC₅₀ / CC₅₀). ^e EC₅₀ indicate half maximal effective concentration on extracellular *L. donovani*. Average of duplicate determinations. ^f N/A, not available. ^g N/T, not tested.

Table 3. *In vitro* activity of 2,3-dihydroimidazo[1,2-*a*]benzimidazole derivatives against intracellular *T. cruzi*

Compound	Activity against <i>T. cruzi</i>		
	EC ₅₀ (μM) ^a	CC ₅₀ (μM) ^b	SI ^c
3	> 50	> 50	N/A ^d
4	1.10	36.5	33.2
5	3.09	> 50	> 16.2
6	36.0	> 50	> 1.39
7	8.70	37.9	4.36
8	12.7	21.0	1.65
9	8.24	50.0	6.07
10	6.21	5.18	0.8
11	19.6	44.6	2.28
12	> 50	> 50	N/A
14	33.7	> 50	> 1.48
15	> 50	> 50	N/A
16	1.60	6.10	3.81
17	> 50	> 50	N/A
18	12.5	34.6	2.77
20	> 50	> 50	N/A
21	13.4	> 50	> 3.75
24	2.10	18.8	8.95
25	4.49	9.61	2.14
26	8.89	> 50	> 5.62
27	7.45	10.3	1.38
28	> 50	> 50	N/A
29	5.56	9.36	1.7
30	> 50	> 50	N/A
31	> 50	> 50	N/A
32	38.7	20.0	0.52
33	> 50	> 50	N/A
Benznidazole	20.7	> 50	> 2.42

^aEC₅₀ indicate half maximal effective concentration on intracellular *T. cruzi* (2-fold dilution with 10 points dose response). ^bCC₅₀ indicate cytotoxicity against U2OS cell, which was determined by counting U2OS cell number in the taken image from intracellular *T. cruzi* assay. ^cSI is selective index (EC₅₀ / CC₅₀). ^dN/A, not available.

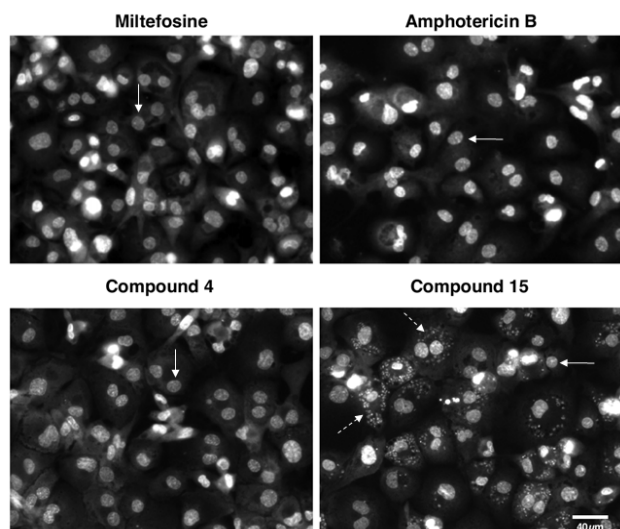


Fig. 1. Confocal microscopy images of intracellular *L. donovani* treated with compounds **4** and **15**: Treatment of compound **4** as well as reference drugs, miltefosine and amphotericin B, at 12.5 μM concentration to intracellular *Leishmania* showed complete parasite clearance from the host cells, THP-1. Treatment of inactive compound **15** showed full of parasites inside at the same concentration. Fluorescent DNA dye, DRAQ5TM, was used to visualize host cells and parasites. The solid arrow indicates nucleus of THP-1 cells and the dotted arrow indicates *Leishmania* in cytosol.

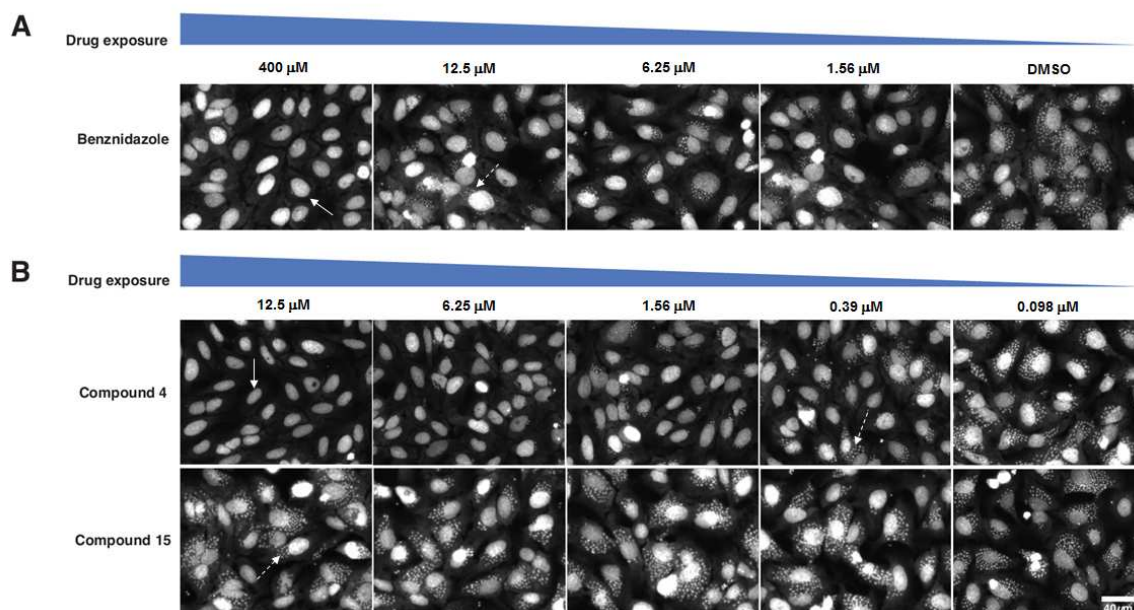


Fig. 2. Confocal microscopy images of intracellular *T. cruzi* treated with compounds **4** and **15**: (A) 400 μM of benznidazole was used as a positive control, and 1 % of DMSO was used as a negative control for the assay. Infected U2OS cells in the presence of 400 μM of benznidazole showed complete parasite clearance from the host cells, while parasites still remained at the concentration of 12.5 μM . (B) Compound **4** showed host clearance of parasite in a dose-dependent manner unlike inactive compound **15**. Fluorescent DNA dye, DRAQ5TM, was used to visualize DNA of host cells and parasites. The solid arrow indicates nucleus and the dotted arrow indicates *T. cruzi* in cytosol.

Figure Caption

Fig. 1. Confocal microscopy images of intracellular *L. donovani* treated with compounds **4** and **15**: Treatment of compound **4** as well as reference drugs, miltefosine and amphotericin B, at 12.5 μM concentration to intracellular *Leishmania* showed complete parasite clearance from the host cells, THP-1. Treatment of inactive compound **15** showed full of parasites inside at the same concentration. Fluorescent DNA dye, DRAQ5TM, was used to visualize host cells and parasites. The solid arrow indicates nucleus of THP-1 cells and the dotted arrow indicates *Leishmania* in cytosol.

Fig. 2. Confocal microscopy images of intracellular *T. cruzi* treated with compounds **4** and **15**: (A) 400 μM of benznidazole was used as a positive control, and 1 % of DMSO was used as a negative control for the assay. Infected U2OS cells in the presence of 400 μM of benznidazole showed complete parasite clearance from the host cells, while parasites still remained at the concentration of 12.5 μM . (B) Compound **4** showed host clearance of parasite in a dose-dependent manner unlike inactive compound **15**. Fluorescent DNA dye, DRAQ5TM, was used to visualize DNA of host cells and parasites. The solid arrow indicates nucleus and the dotted arrow indicates *T. cruzi* in cytosol.

Scheme 1. Reagents and conditions: (A) $\text{R}^3\text{CH}_2\text{Br}$ 1.3 eq, K_2CO_3 1.3 eq, DMF, 120 $^\circ\text{C}$, 4 h; (B) H_2 , 10 % Pd/C, MeOH, RT, 3 h; (C) urea 2.0 eq, DMF, 200 $^\circ\text{C}$, 30 min; (D) POCl_3 10.0 eq, conc. HCl (cat.), 150 $^\circ\text{C}$, 3 h; (E) ethanolamine 10.0 eq, microwave irradiation, 200 $^\circ\text{C}$, 30 min; (F) POCl_3 10.0 eq, 110 $^\circ\text{C}$, 2 h; (G) TEA 1.0 eq, toluene, 110 $^\circ\text{C}$, 8 h; (H) $\text{R}^3\text{CH}_2\text{Br}$ 1.0 eq, DIPEA 1.5 eq, DMF, 100 $^\circ\text{C}$, 12 h.

Scheme 2. Reagents and conditions: (A) Ethanolamine 10.0 eq, microwave irradiation, 200 $^\circ\text{C}$, 30 min; (B) 2-bromo-4'-*tert*-butylacetophenone 1.0 eq, DMF, 15 h; (C) POCl_3 10.0 eq, 110 $^\circ\text{C}$, 2 h; (D) TEA 1.0 eq, toluene, 110 $^\circ\text{C}$, 8 h; (E) 2-bromo-4'-*tert*-butylacetophenone 1.0 eq, DIPEA 1.5 eq, DMF, 100 $^\circ\text{C}$, 8 h.

Highlights

- HTS/HCS campaign was performed to identify anti-leishmanial and anti-*T. cruzi* agents.
- 2,3-Dihydroimidazo[1,2-*a*]benzimidazole was a novel scaffold of anti-parasitic agents.
- Synthetic analogues were tested against intracellular and extracellular parasite forms.
- **4** and **24** showed superior anti-trypanosomal activity compared to current drugs.

< Supplementary Information >

Synthesis and biological evaluation of 2,3-dihydroimidazo[1,2-*a*]benzimidazole derivatives against *Leishmania donovani* and *Trypanosoma cruzi*

Sangmi Oh,^a Sungbum Kim,^a Sunju Kong,^a Gyongseon Yang,^b Nakyung Lee,^b Dawoon Han,^b
Junghyun Goo,^b Jair L. Siqueira-Neto,^{b,†} Lucio H. Freitas-Junior,^{b,‡} Michel Liuzzi,^c Jinhwa
Lee,^d Rita Song^{a,*}

^a Medicinal Chemistry Group, Institut Pasteur Korea, 696 Sampyeong-dong, Bundang-gu, Seongnam-si, Gyeonggi-do 463-400, Korea

^b Center for Neglected Diseases Drug Discovery (CND3), Institut Pasteur Korea, 696 Sampyeong-dong, Bundang-gu, Seongnam-si, Gyeonggi-do 463-400, Korea

^c Early Discovery Program, Institut Pasteur Korea, 696 Sampyeong-dong, Bundang-gu, Seongnam-si, Gyeonggi-do 463-400, Korea

^d Late Discovery Program, Institut Pasteur Korea, 696 Sampyeong-dong, Bundang-gu, Seongnam-si, Gyeonggi-do 463-400, Korea

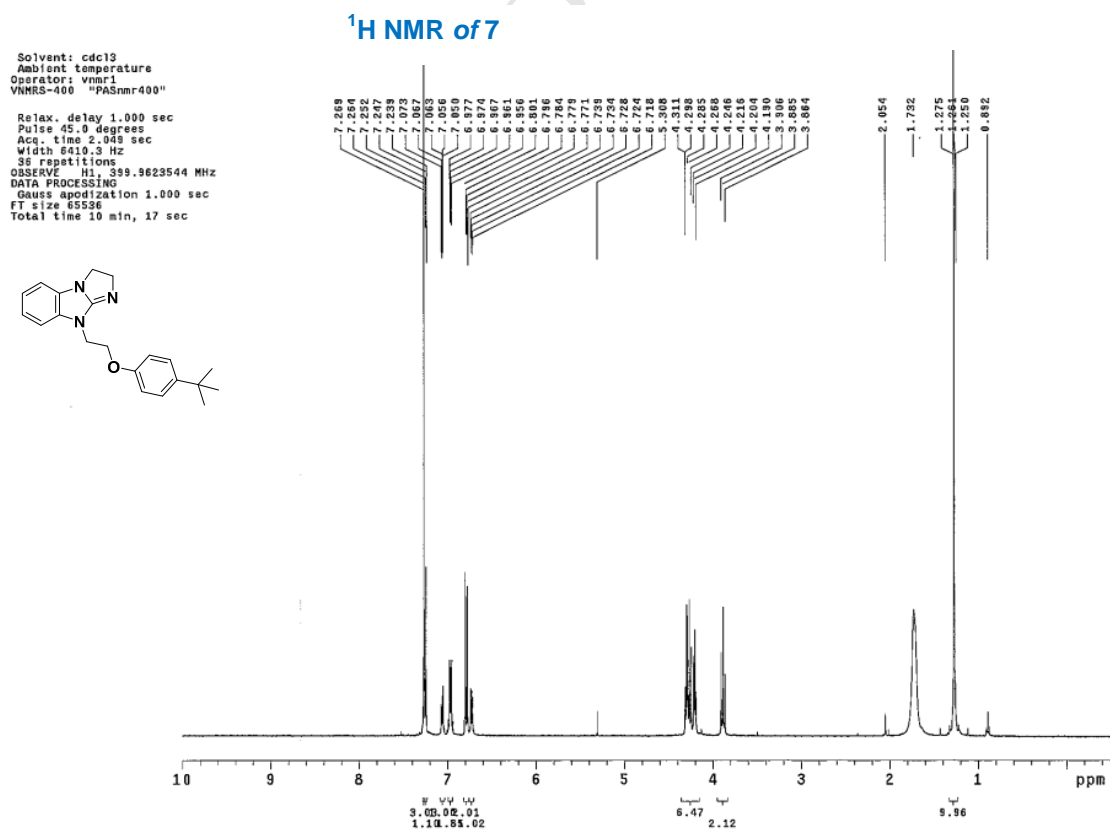
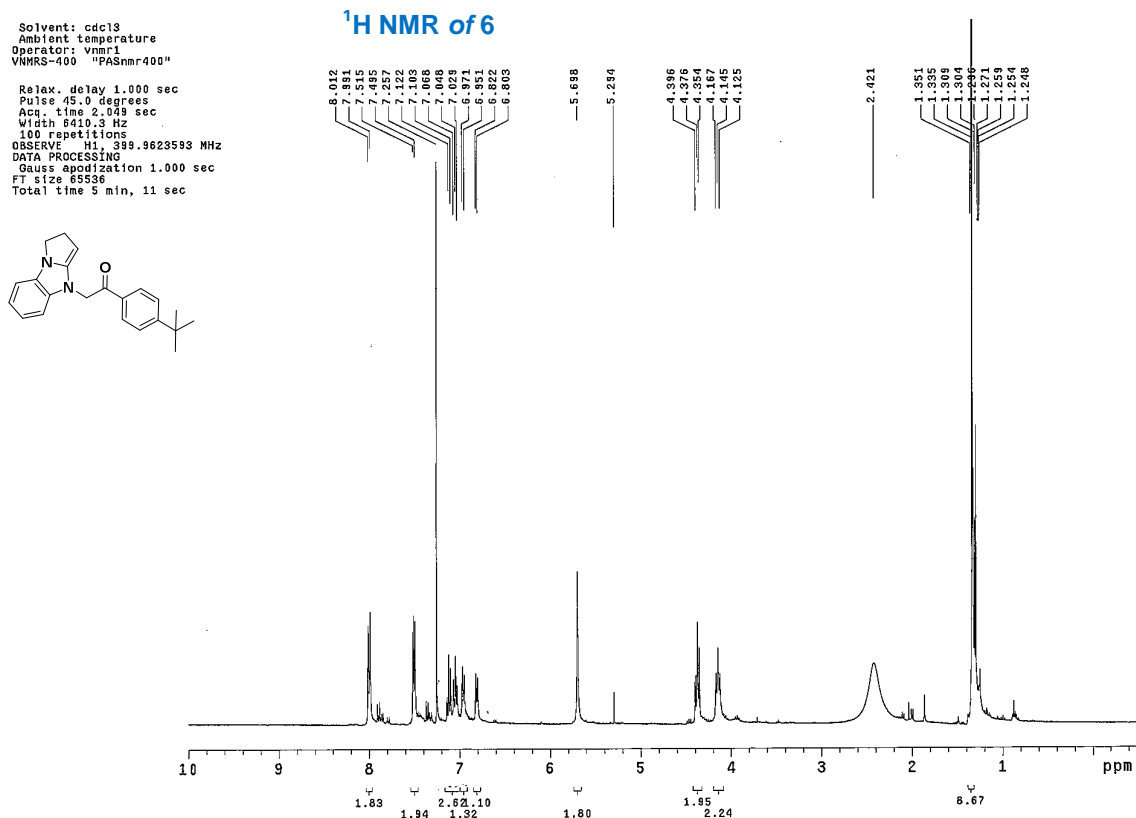
[†] Present address: University of California, San Francisco, USA

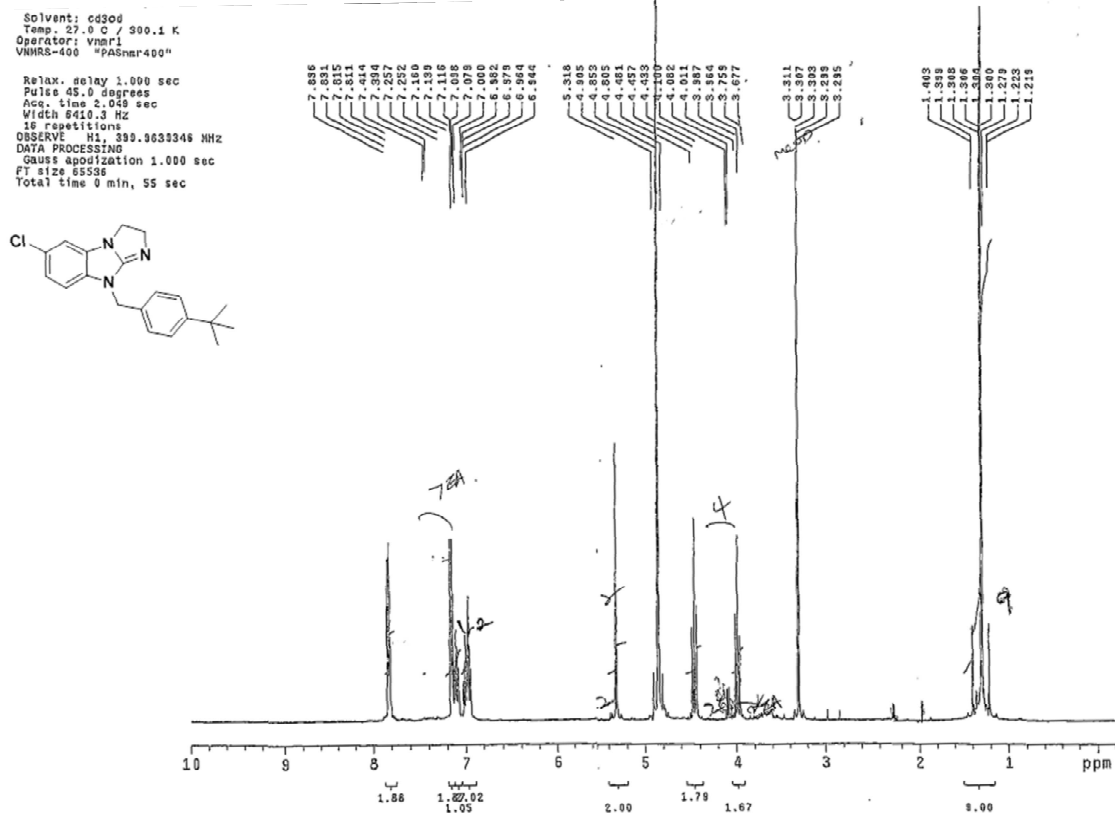
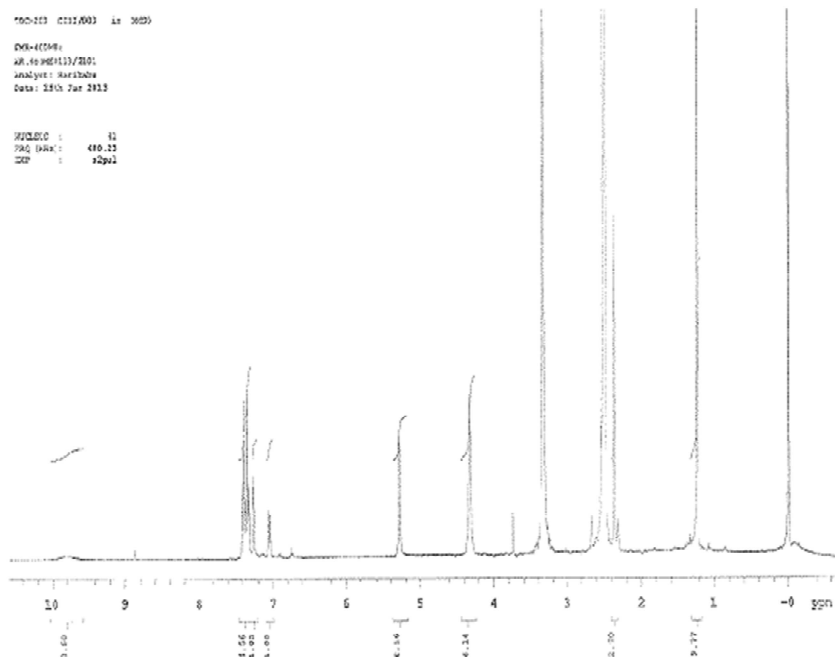
[‡] Present address: Laboratório Nacional de Biociências (LNBio), Brazil

* Corresponding author

Tel.: +82-31-8018-8230; fax: +82-31-8018-8014; e-mail: rsong@ip-korea.org

I. NMR Data of Newly Synthesized Compounds

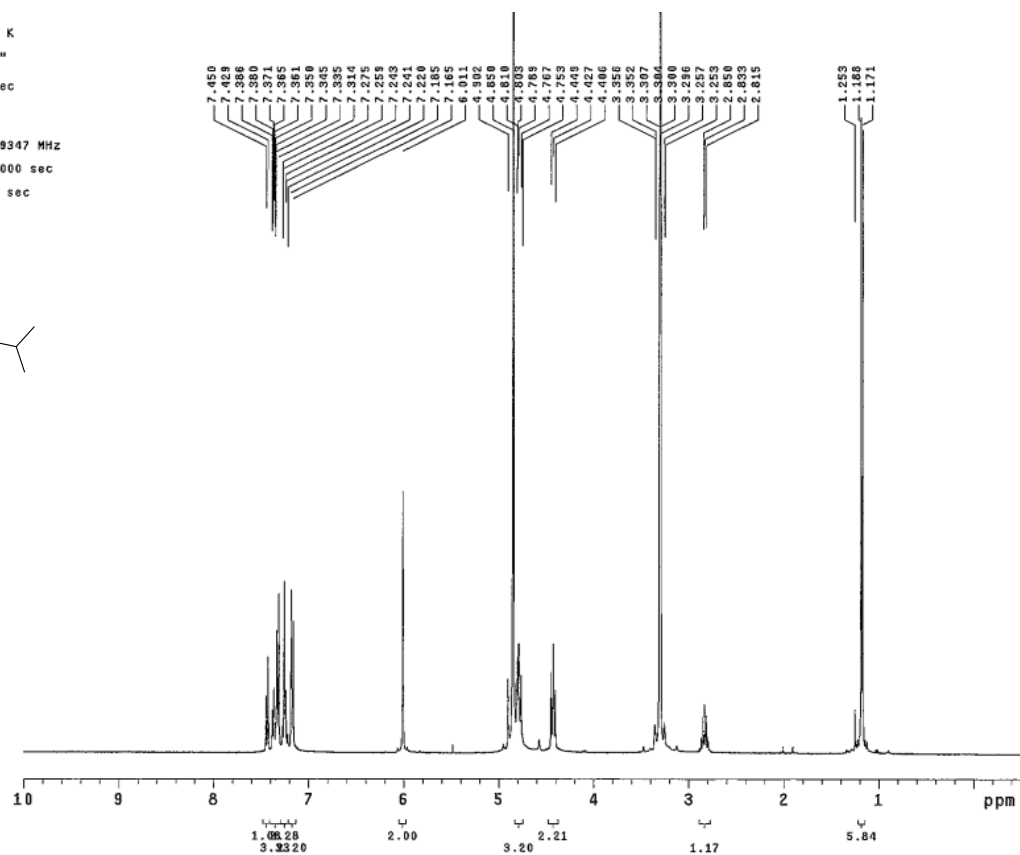
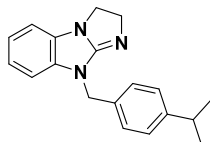


¹H NMR of 10¹H NMR of 11

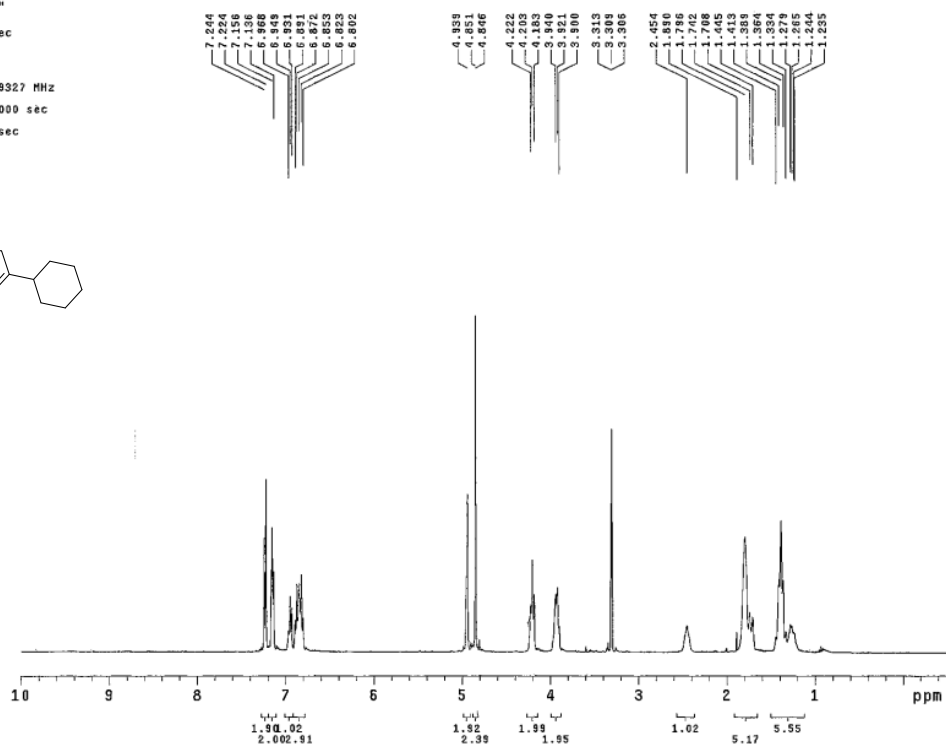
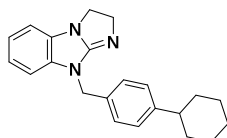
¹H NMR of 9-(4-(tert-butyl)benzyl)-6-methyl-3,9-dihydro-2H-benzod[imidazo[1,2-a]imidazole (CIBI/003):

¹H NMR of 15

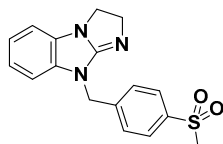
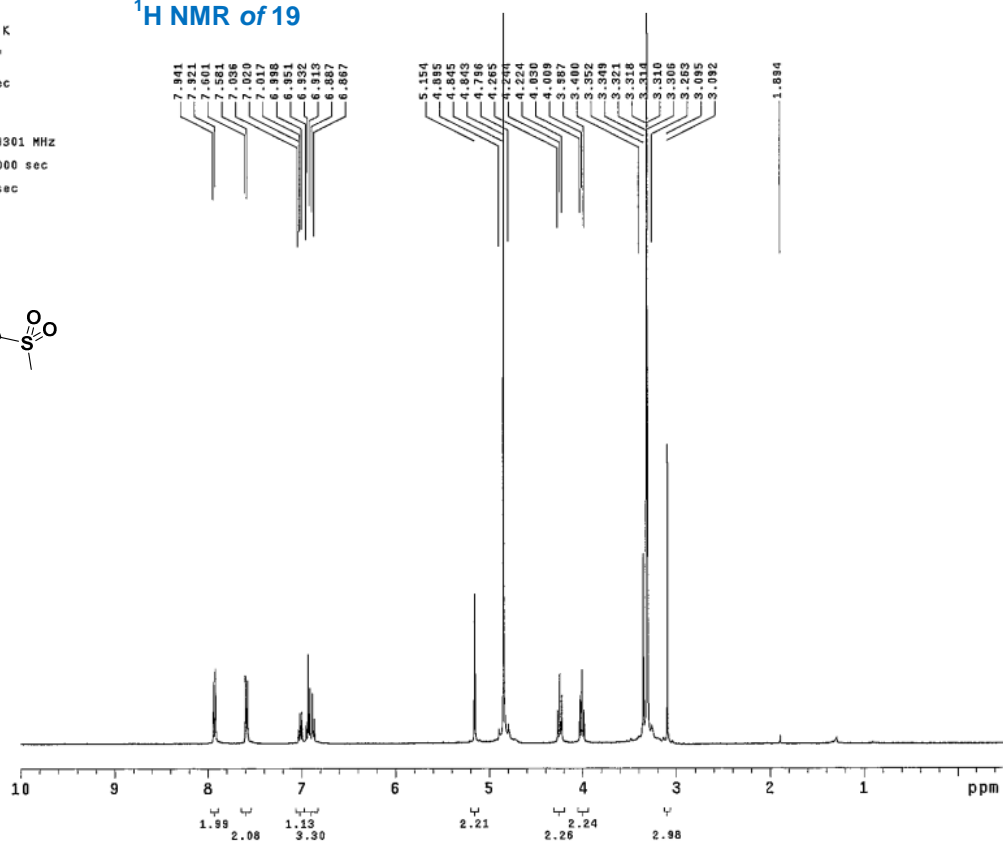
Solvent: cd3od
 Temp. 26.0 C / 299.1 K
 Operator: vnmr1
 VNMRS-400 "PASnmr400"
 Relax. delay 1.000 sec
 Pulse 45.0 degrees
 Acq. time 2.049 sec
 Width 6410.3 Hz
 34 repetitions
 OBSERVE H1, 399.9639347 MHz
 DATA PROCESSING
 Gauss apodization 1.000 sec
 FT size 65536
 Total time 10 min, 17 sec

¹H NMR of 16

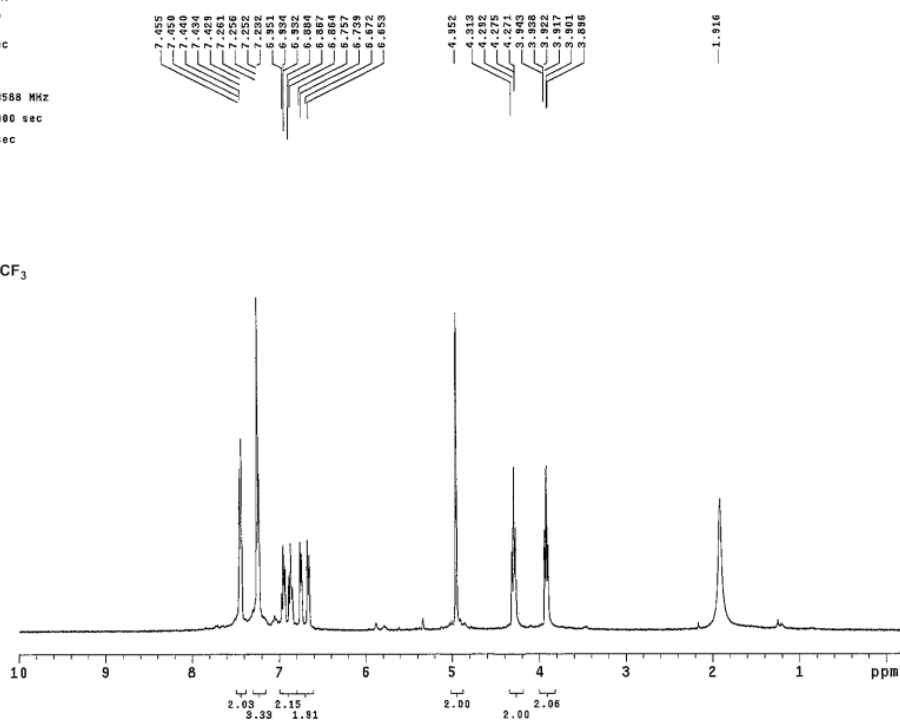
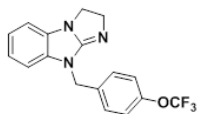
Solvent: cd3od
 Temp. 26.0 C / 299.1 K
 Operator: vnmr1
 VNMRS-400 "PASnmr400"
 Relax. delay 1.000 sec
 Pulse 45.0 degrees
 Acq. time 2.049 sec
 Width 6410.3 Hz
 72 repetitions
 OBSERVE H1, 399.9639327 MHz
 DATA PROCESSING
 Gauss apodization 1.000 sec
 FT size 65536
 Total time 5 min, 11 sec



Solvent: cd3od
 Temp. 26.0 C / 299.1 K
 Operator: vnmr1
 VNMR-400 "PASnmr400"
 Relax. delay 1.000 sec
 Pulse 45.0 degree
 Acq. time 2.049 sec
 Width 6410.3 Hz
 32 repetitions
 OBSERVE H1 399.9639301 MHz
 DATA PROCESSING
 Gauss apodization 1.000 sec
 FT size 65536
 Total time 5 min, 11 sec

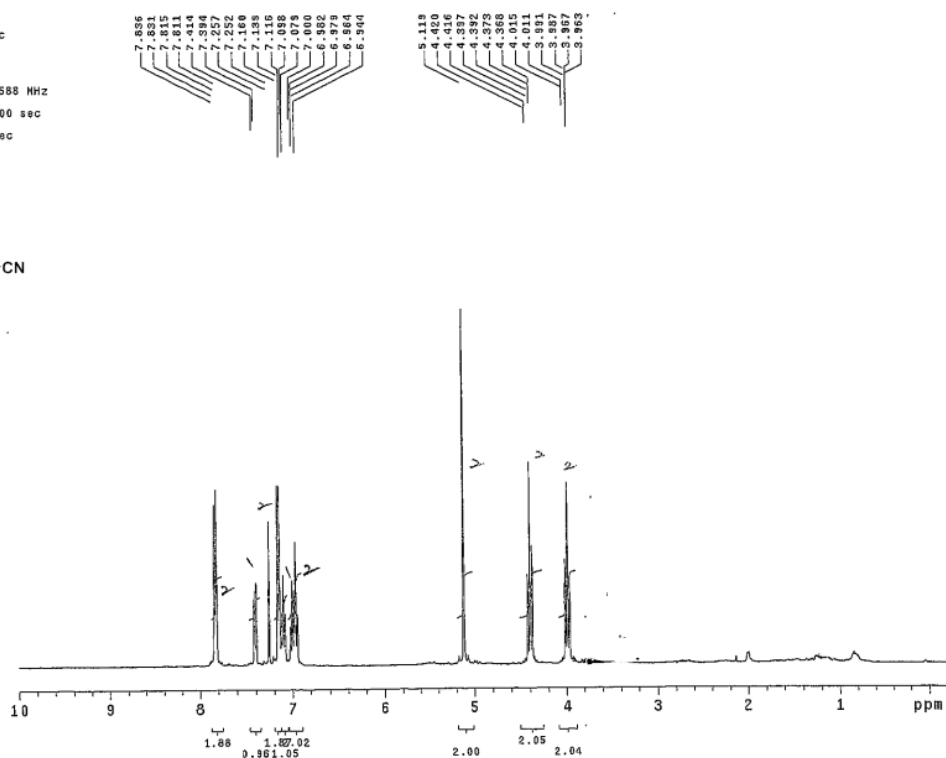
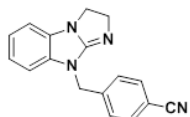
¹H NMR of 19¹H NMR of 22

Solvent: cdcl3
 Temp. 27.0 C / 300.1 K
 Operator: vnmr1
 VNMR-400 "PASnmr400"
 Relax. delay 1.000 sec
 Pulse 45.0 degree
 Acq. time 2.049 sec
 Width 6410.3 Hz
 16 repetitions
 OBSERVE H1 399.9623588 MHz
 DATA PROCESSING
 Gauss apodization 1.000 sec
 FT size 65536
 Total time 0 min, 55 sec

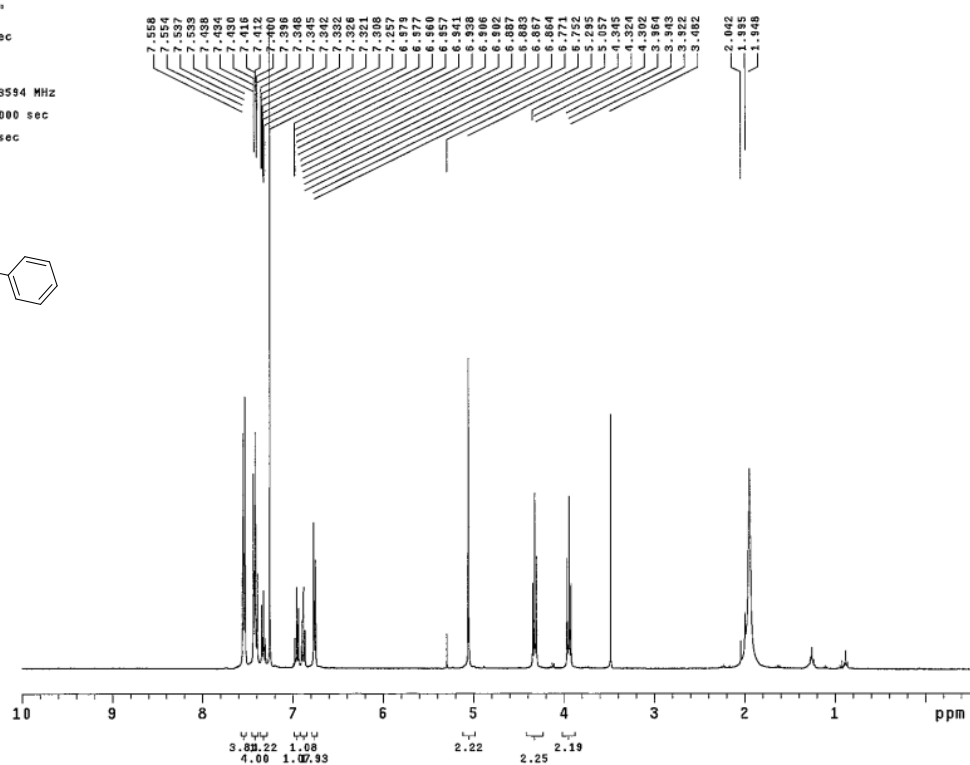
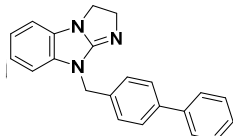


¹H NMR of 23

Solvent: cdcl3
 Temp. 27.0 C / 300.1 K
 Operator: vnmr1
 VNMR-400 "PASNmr400"
 Relax. delay 1.000 sec
 Pulse 45.0 degrees
 Acq. time 2.049 sec
 Width 6410.3 Hz
 16 repetitions
 OBSERVE H1, 399.9623588 MHz
 DATA PROCESSING
 Gauss apodization 1.000 sec
 FT size 65536
 Total time 0 min, 55 sec

¹H NMR of 24

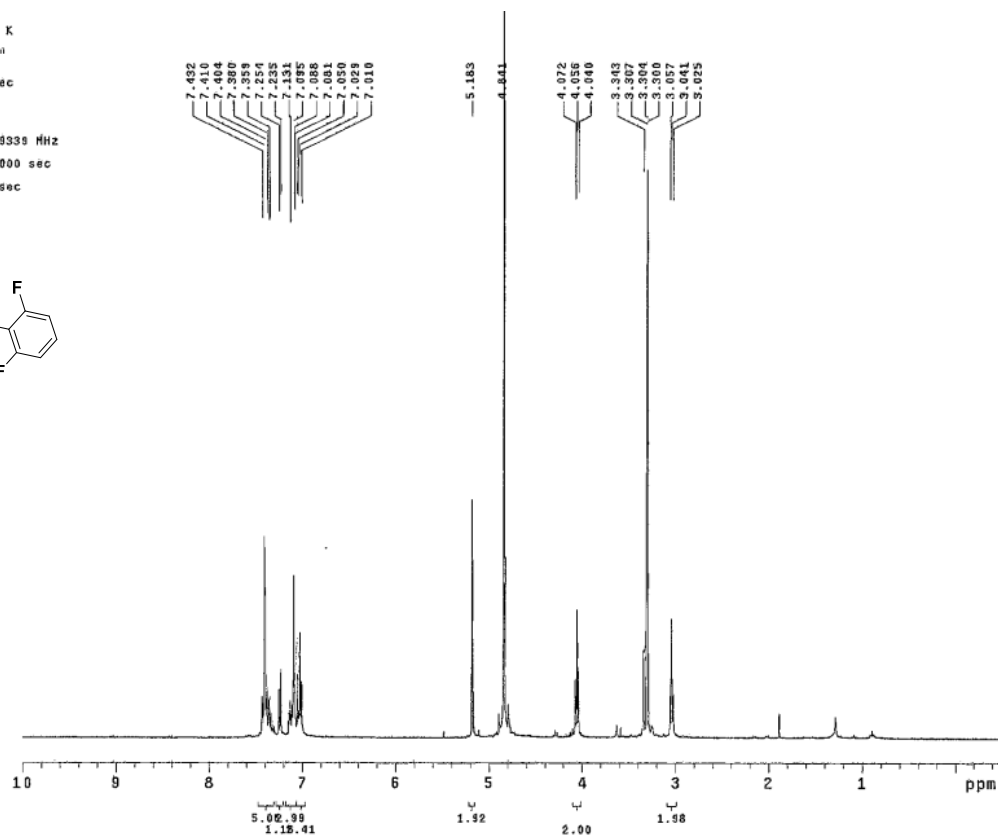
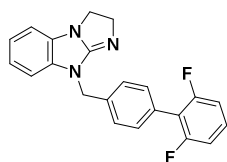
Solvent: cdcl3
 Ambient temperature
 Operator: vnmr1
 VNMR-400 "PASNmr400"
 Relax. delay 1.000 sec
 Pulse 45.0 degrees
 Acq. time 2.049 sec
 Width 6410.3 Hz
 50 repetitions
 OBSERVE H1, 399.9623594 MHz
 DATA PROCESSING
 Gauss apodization 1.000 sec
 FT size 65536
 Total time 5 min, 11 sec



¹H NMR of 25

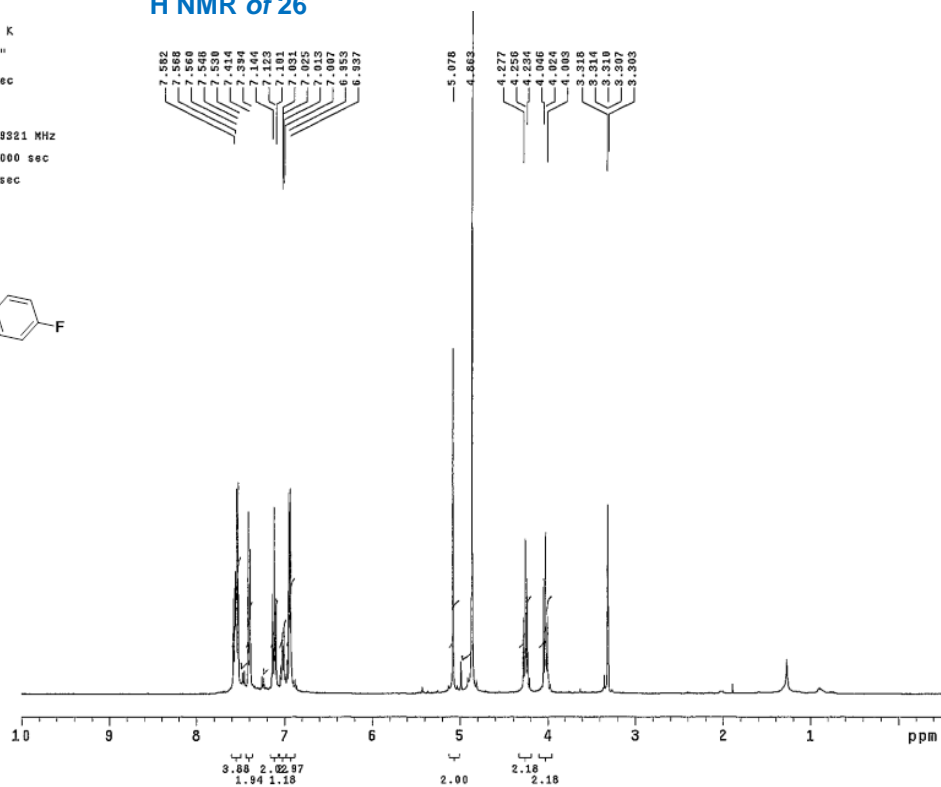
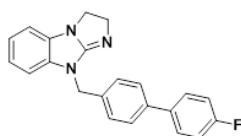
Solvent: cd3od
 Temp. 26.0 C / 299.1 K
 Operator: vnmr1
 VNMRS-400 ¹HASnmr400"

Relax. delay 1.000 sec
 Pulse 45.0 degrees
 Acq. time 2.049 sec
 Width 6419.3 Hz
 26 repetitions
 OBSERVE H1, 399.9639339 MHz
 DATA PROCESSING
 Gauss apodization 1.000 sec
 FT size 65536
 Total time 5 min, 11 sec

¹H NMR of 26

Solvent: cd3od
 Temp. 27.0 C / 300.1 K
 Operator: vnmr1
 VNMRS-400 ¹HASnmr400"

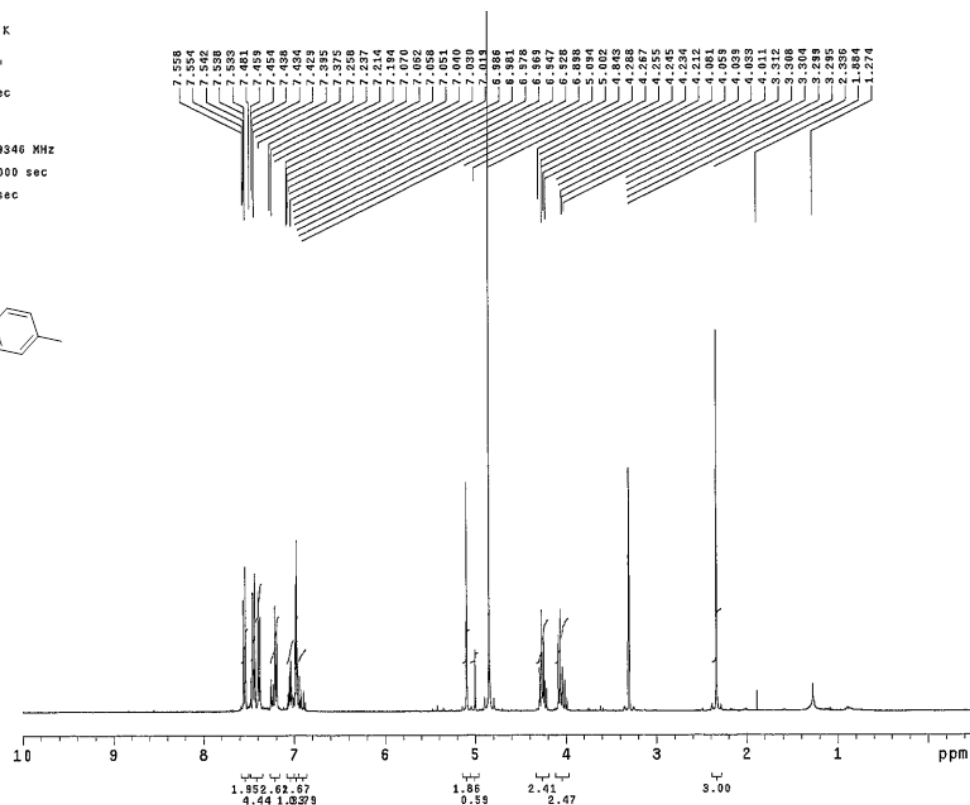
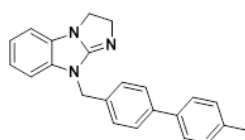
Relax. delay 1.000 sec
 Pulse 45.0 degrees
 Acq. time 2.049 sec
 Width 6419.3 Hz
 16 repetitions
 OBSERVE H1, 399.9639321 MHz
 DATA PROCESSING
 Gauss apodization 1.000 sec
 FT size 65536
 Total time 0 min, 55 sec



¹H NMR of 27

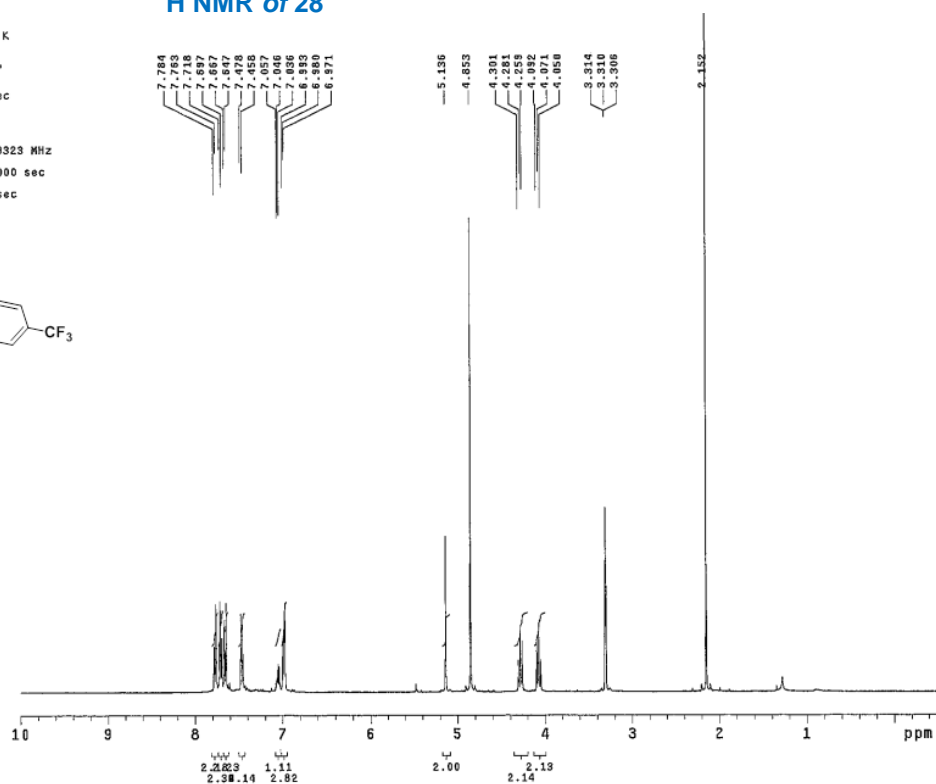
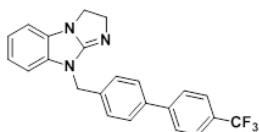
Solvent: cd3od
 Temp: 27.0 C / 300.1 K
 Operator: vnmr1
 File: 590-K8B-187
 VNMRS-400 "PASCNMR400"

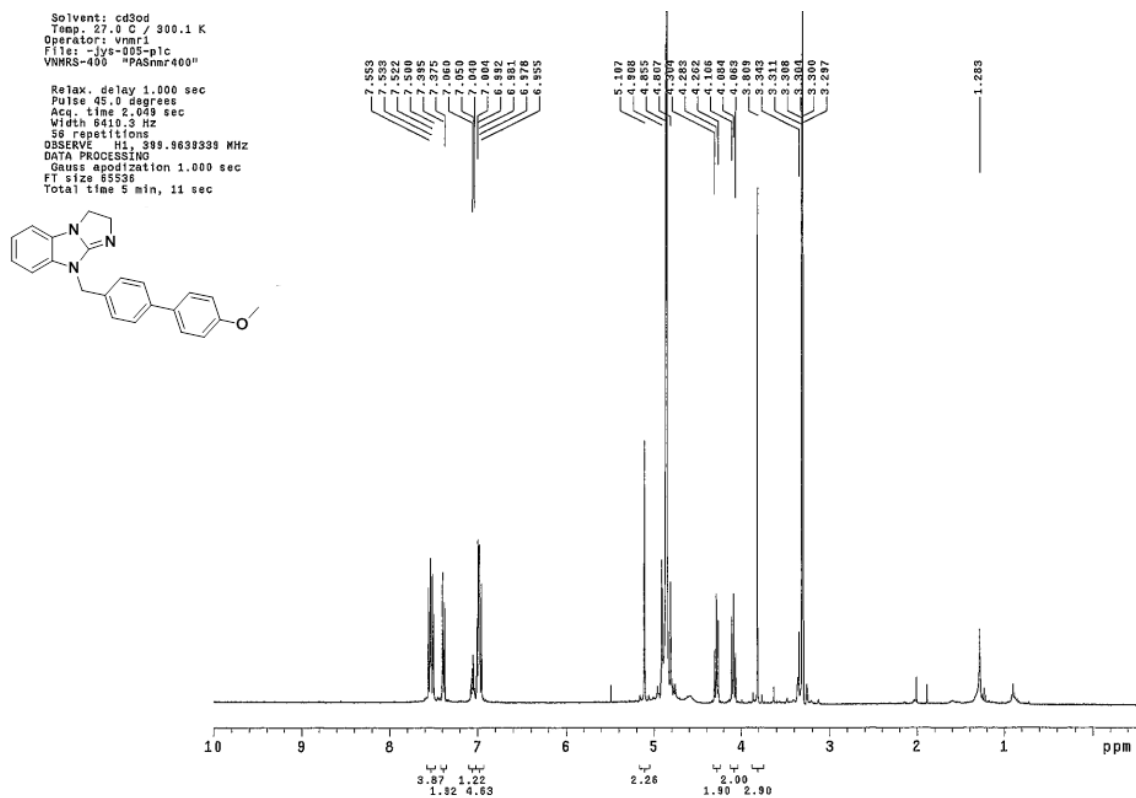
Relax. delay 1.000 sec
 Pulse 45.0 degrees
 Acq. time 2.049 sec
 Width 6410.3 Hz
 16 repetitions
 OBSERVE H1 399.9639340 MHz
 DATA PROCESSING
 Gauss apodization 1.000 sec
 FT size 65536
 Total time 0 min, 55 sec

¹H NMR of 28

Solvent: cd3od
 Temp: 27.0 C / 300.1 K
 Operator: vnmr1
 File: 590-K8B-188
 VNMRS-400 "PASCNMR400"

Relax. delay 1.000 sec
 Pulse 45.0 degrees
 Acq. time 2.049 sec
 Width 6410.3 Hz
 16 repetitions
 OBSERVE H1 399.9639323 MHz
 DATA PROCESSING
 Gauss apodization 1.000 sec
 FT size 65536
 Total time 0 min, 55 sec



¹H NMR of 31¹H NMR of 32